

# Time-Evolving Psychological Processes Over Repeated Decisions

David Gunawan<sup>1</sup>, Guy E. Hawkins<sup>2</sup>, Robert Kohn<sup>3</sup>, Minh-Ngoc Tran<sup>4</sup>, Scott D. Brown<sup>2</sup>

1: School of Mathematics and Applied Statistics, University of Wollongong

2: School of Psychology, University of Newcastle, Australia

3: Australian School of Business, University of New South Wales, Sydney, Australia

4: Discipline of Business Analytics, University of Sydney Business School

## Abstract

Many psychological experiments have participants repeat a simple task. This repetition is often necessary in order to gain the statistical precision required to answer questions about quantitative theories of the psychological processes underlying performance. In such experiments, time-on-task can have sizable effects on performance, changing the psychological processes under investigation in interesting ways. These changes are often ignored, and the underlying process is treated as static. We propose modern statistical approaches that are based on recent advances in particle Markov chain Monte-Carlo (MCMC) to extend a static model of decision-making to account for time-varying changes in a psychologically plausible manner. Using data from three highly-cited experiments we show that there are changes in performance with time-on-task, and that these changes vary substantially over individuals. We find strong evidence in favor of a hidden Markov switching process as an explanation of time-varying effects. This embodies the psychological assumption that participants switch between different cognitive states, representing different modes of decision-making, and explains key long- and short-term dynamic effects in the data. The central idea of our approach can be applied quite generally to quantitative psychological theories, beyond the models and data sets that we investigate.

*Keywords:* dynamic; decision making; fatigue; hidden Markov process; practice; time-on-task

---

This research was partially supported by the Australian Research Council (ARC) Discovery Project scheme (DP180102195, DP180103613). Hawkins was partially supported by an ARC Discovery Early Career Researcher Award (DECRA; DE170100177). Earlier versions of this work were posted online at <https://arxiv.org/abs/1906.10838> and presented at the 2019 meetings of the Psychonomic Society and the Australasian Mathematical Psychology Conference.

A standard feature of almost all experiments in cognitive psychology is repetition: participants make repeated responses to very similar (or even identical) stimuli for an extended period of time. This repetition is an important way to increase the size of the data sample and reduce measurement noise, and is often traded off against the number of participants from whom data are collected. In paradigms where little variation is expected between participants (e.g., some aspects of vision), many thousands of observations are collected from just a handful of people. In other experiments where large variation is expected between people (e.g., social attitudes), a small number of data are collected from many hundreds of participants.

Figure 1 illustrates data from a typical experiment – a neuropsychological investigation of decision-making reported by Forstmann et al. (2008), in which participants made several hundred decisions. The figure shows the data differently from the many other analyses reported elsewhere for this experiment, making it clear that the basic properties of participants’ decisions change substantially over the course of the experiment. The left panels of Figure 1 show that the average accuracy of decisions decreases with time-on-task, while both the average response time (RT) and its variability increases. The data for individual participants is even more variable; the right panels of the figure show the data for three participants. Different individuals certainly show different-sized effects of time-on-task, but they also appear to have different qualitative directions of the effect. For example, the top right panel of the figure shows that average accuracy is approximately stable for one participant, decreases with time-on-task for another, and increases with time-on-task for the third. Changes with practice are to be expected, because psychological experiments are both difficult and taxing. Participants learn to be better at the task, but they also suffer from fatigue, boredom, and many other unpredictable effects. It is clearly unreasonable to assume that identical cognitive processes underlie each repeated decision.

The magnitude of the changes with time-on-task may be surprising. In Figure 1, the average accuracy of decisions declines from about 90% at the start of the experiment to just above 80% at the end. This effect has similar size as the key experimental manipulation studied by Forstmann et al. (2008). Even with this substantial practice, the average RT and accuracy are still clearly changing by the end of the session. Some experiments include even more practice than that – we investigate two examples of this later. In some of these cases we observe stable group summary statistics, like mean accuracy and RT, after sufficient practice. However, even this does not imply that any individual’s performance is constant. This is the same problem associated with averaging that arises in most analyses. Our investigations (see Figures 4 and A1 below, for example) suggest that most participants continue to change substantially on either, or both, of mean RT and accuracy even up to 2,000 trials of practice.

Large changes with time-on-task can be observed in almost any psychological experiment. There have been some efforts to understand the psychological causes of these changes, such as in studies of the effects of extended practice (Evans, Brown, Mewhort, & Heathcote, 2018; Heathcote, Brown, & Mewhort, 2000; A. Newell & Rosenbloom, 1981; Palmeri, 1999), of fatigue (Ratcliff & Van Dongen, 2011; Walsh, Gunzelmann, & Van Dongen, 2017), or “mind wandering” (Christoff, Irving, Fox, Spreng, & Andrews-Hanna, 2016; Mittner, Hawkins, Boekel, & Forstmann, 2016). Those researchers sought to understand changes over time in psychologically meaningful ways by applying time-varying quanti-

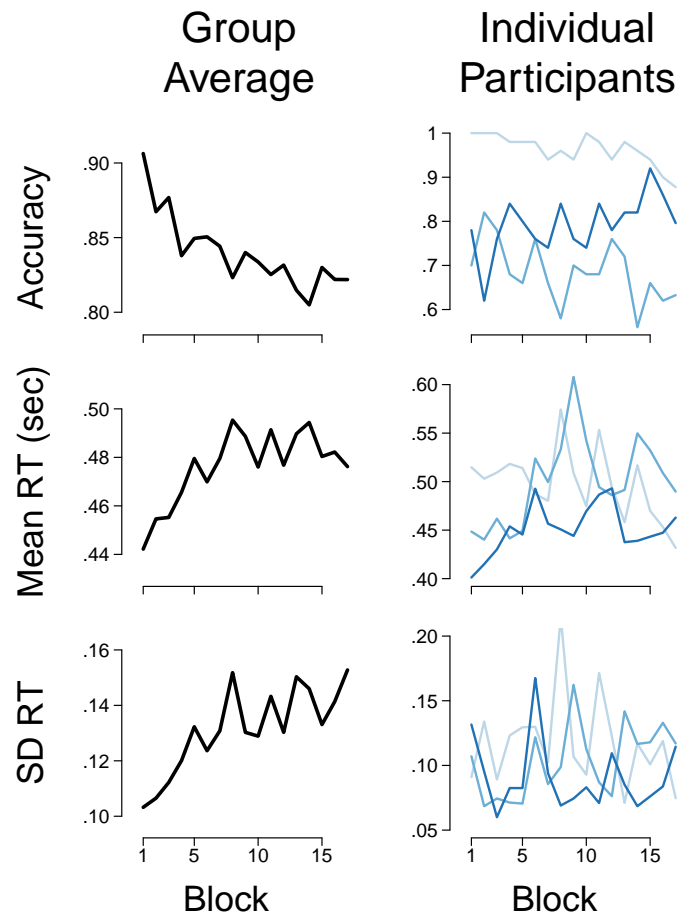


*Figure 1.* Data from Forstmann et al. (2008). Participants make repeated decisions about simple stimuli, but the effects of practice are complex and varied. The top row shows that accuracy in those decisions decreases with time-on-task ( $x$ -axis) in the aggregate (left panels), but this trend is inconsistent across three exemplar participants (separate lines, right panels). The middle panels show that mean response time (RT) across participants increases with practice, but the same three individual participants show a mix of increasing or decreasing RT with practice. Similarly complex trends are apparent in the variance of RT (bottom panels).

tative models to the data. This can be difficult, because the quantitative modelling of time-varying data presents challenging computational and statistical problems. This leaves open scientifically interesting questions about how time-on-task interacts with important psychological processes. For example, time-on-task might be expected to change the engagement of participants with the experiment, or the features of the stimuli to which they pay attention. Instead of investigating such questions, a typical approach simply ignores the effects of time-on-task, and averages across data from different periods of the experiment. When dynamic effects are obvious or large, some researchers remove data from early time periods (a few trials, blocks, or sessions), and then average over the remaining data. Both approaches are problematic on two levels: methodologically, there is the problem of the clearly unjustified model assumption of identical data-generating processes across time; and scientifically, there is the potential to miss important aspects of psychological change over time.

While the theoretical questions raised by the effects of time-on-task are interesting, an important reason why they receive little attention is practical: including time-varying effects in quantitative psychological theories is difficult. This is evident, for example, in the difficulty of addressing important and widely-recognized questions about the moment-to-moment “sequential effects” in behavioral data. Sequential effects refer to the micro-structure of dynamic effects, where participants’ responses are strongly influenced by their experiences and behavior in the preceding few seconds; e.g., Brown, Marley, Donkin, and Heathcote (2008); Craigmile, Peruggia, and Van Zandt (2010); Kim, Potter, Craigmile, Peruggia, and Van Zandt (2017). Traditional approaches to modelling dynamic effects either require strong assumptions prescribing the way in which behavior changes over time, or require splitting the data into smaller and smaller segments, bringing the usual problems associated with small samples. We now illustrate with example the limitations of these approaches. A. Newell and Rosenbloom (1981), Heathcote et al. (2000) and Evans et al. (2018) investigated how the performances of simple skills (e.g., rolling cigars, memorizing rules, ...) improve with practice. The researchers took a “strong assumptions” approach, by identifying a few candidate functions that might describe how performance changes with practice, and comparing those functions against the data. This approach is tractable and powerful, but there are severe limits imposed by the particular functions that are chosen for comparison. Their investigations focus primarily on the comparison of just two theories about how performance changes with practice (exponential and power functions). The approach is difficult to extend to very many comparison functions. Furthermore, each function considered represents a strong theory about changes with practice. For example, the power and exponential functions both insist that all participants improve with practice, and that the rate of improvement decreases with time-on-task. These assumptions might be defensible in some paradigms, but are probably unreasonable more generally. The assumptions are also inconsistent with what is known about individual differences. For example, how will these analyses interact with the inevitable participant who gets worse with practice, or who improves in a step function manner? Even more likely, how will these analyses interact with the inevitable mind-wandering that occurs during extended tasks, in which participants intermittently switch between different more and less engaged states?

As an example of the other type of approach mentioned above, Evans and Hawkins (2019) investigated how extended practice might explain differences between humans and

monkeys in a decision-making paradigm. Evans and Hawkins investigated time-on-task by splitting the data from each participant into periods defined by the design (different sessions of practice, from different days). This approach is reasonable for their experiment, where the number of data were very large. Even after splitting the data into 10 blocks, there were still many hundreds of data in each block, allowing reliable analysis. For more typical designs, splitting data to investigate time-on-task can lead to unacceptably small sample sizes. Beyond the problem of sample size, investigating time by splitting data into different time periods treats data from these periods as independent and stationary within periods. Both of these assumptions are clearly unreasonable – data from the first session of practice are more likely to be similar to data from the second session of practice than to data from the final session of practice. Within each session, there are likely to be warm-up effects near the start, as well as periods of fluctuating attention and focus. Failing to account for these dynamic effects makes the approach both less satisfactory as an explanatory process, and also weakens its statistical power.

### A New Approach

We propose advancing scientific approaches to time-on-task effects by incorporating recent advances in statistical modeling and estimation. The key idea is to model dynamic changes by allowing the parameters of a cognitive model to change with time-on-task according to flexible but statistically tractable dynamic models. Our approach combines advantages of previous methods, such as coherently pooling information across different times, while avoiding some of the limitations, such as assuming independence between times, or assuming rigid functional forms for the time effects.

We illustrate and test our methods using data from three experiments: the one discussed above (Forstmann et al., 2008) and two reported by Wagenmakers, Ratcliff, Gomez, and McKoon (2008). We adopt a hierarchical Bayesian approach to the analysis, with each participant having a unique set of parameters for a cognitive model of the task, and constrain these parameters to follow a parametric distribution across participants. We explore three different accounts of dynamic change and the micro-structure of decision-making. For two accounts, we allow the parameters of the model to change across time in the experiment, according to simple statistical processes: either smooth polynomial trends, or flexible non-smooth changes described by an autoregressive process. For the third account, we investigate a model motivated by process-level psychological theory. This account encapsulates the idea that participants can make decisions using different modes or “states”, such as on-task and off-task, or more vs. less cautiously. The model explains how participants switch between those different states, using a hidden Markov process. The state-based hidden Markov process is motivated by previous theoretical accounts of mind-wandering (McVay & Kane, 2010; Mittner et al., 2016; Smallwood & Schooler, 2015), which propose that mind wandering occurs in a binary fashion, with unpredictable switches between on-task and off-task states.

The dynamic processes provide constraints on the evolution of random effects across participants, but they do not impose fixed deterministic values for changes with time. This facilitates exploration of the differences between people in changes with time, which are expressed in the posterior estimates. For example, the polynomial trend prior captures the expectation that average trends in random effects are similar across people. The autore-

gressive prior imposes the expectation that the “persistence” (correlation) of random effects from block to block is the same across people. The Markov switching process imposes the expectation that there is a probability of being “off-task” for each person, but does not force this to be identical across people, or across time-on-task. We explore the practical and scientific performance of these assumptions in psychological data. This requires developing new estimation approaches that are based on particle MCMC. While our examples are particular to the data and models we explore, an important contribution of our work is that the statistical approach and the new estimation methods are quite general and likely to be useful in a wide range of investigations.

## Methods

### Modelling Approach

All three data sets considered here consist of repeated simple decisions. It is standard to model such data using evidence accumulation models (Donkin & Brown, 2018; Ratcliff, Smith, Brown, & McKoon, 2016). We use the linear ballistic accumulator (LBA; Brown & Heathcote, 2008), which is a well-established accumulator model that was previously applied to data including those analyzed here. Figure 2 illustrates that the LBA represents a decision between two options (such as “word” vs. “non-word” or “leftward motion” vs. “rightward motion”) as a race between two accumulators. Each accumulator gathers evidence in favor of one of the two responses. The amount of evidence in each accumulator increases with passing decision time, until the evidence in one of the accumulators reaches a threshold amount, triggering a decision response. The model makes quantitative predictions about the joint distribution over response times and decision outcomes. These predictions are specified by the values given to the model’s parameters: the height of the response threshold, the distributions of drift rates and starting points for evidence accumulation, and the amount of time taken by processes outside of the decision itself.

**Standard (Static) LBA Model.** Modern applications of the standard static LBA model use a hierarchical Bayesian implementation. Mostly, these applications have used differential evolution Markov chain Monte-Carlo (MCMC) to estimate the posterior distribution over parameters and random effects (Turner, Sederberg, Brown, & Steyvers, 2013). Our analyses use a more efficient estimation procedure based on particle MCMC methods developed by Gunawan, Hawkins, Tran, Kohn, and Brown (2020). Decisions in the experiments under consideration are always forced choices between two alternatives. For these, the  $i^{th}$  decision for the  $j^{th}$  participant yields two pieces of information. The first is the response choice,  $RE_{ij} \in \{1, 2\}$ . The second is the response time,  $RT_{ij} \in (0, \infty)$ . Assuming that the variance of the drift rate distributions in the LBA model are always  $s^2 = 1$  (see also Donkin, Brown, & Heathcote, 2009), the predictions of the model for any particular decision are defined by a vector of five parameters;  $\{\tilde{b}_j, \tilde{A}_j, \tilde{v}_j^{(1)}, \tilde{v}_j^{(2)}, \tilde{\tau}_j\}$ . Parameter  $\tilde{b}_j$  is the decision threshold adopted by participant  $j$  – the amount of evidence required to trigger a decision. The tilde notation,  $\tilde{b}_j$ , is used to distinguish these parameters, which are restricted to positive values, from the log-transformed ones we work with,  $b_j$ . Parameter  $\tilde{A}_j$  is the width of the uniform distribution of start points for the same participant, and  $\tilde{\tau}_j$  is the amount of time taken by processes other than evidence accumulation (also called the “non-decision time”). The values  $\tilde{v}_j^{(1)}$  and  $\tilde{v}_j^{(2)}$  give the mean of the drift rate distri-

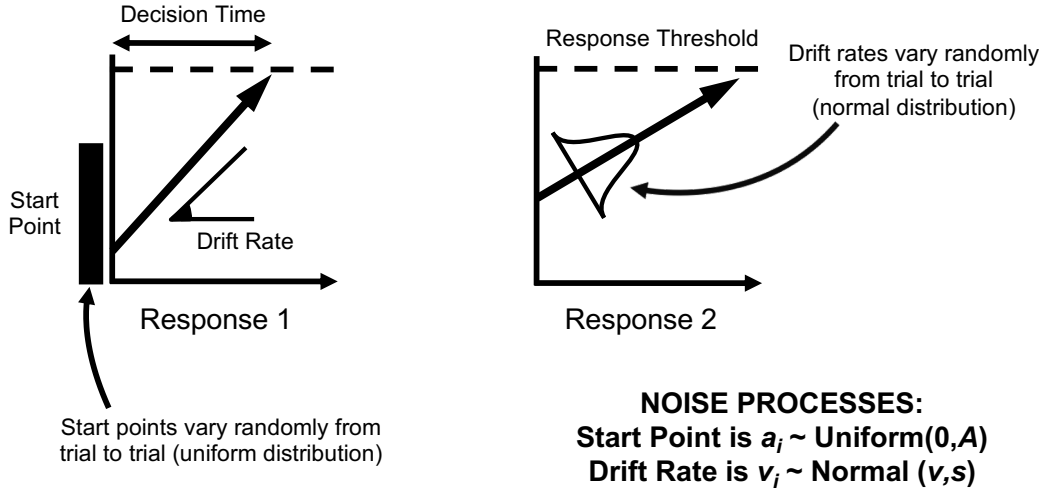


*Figure 2.* The linear ballistic accumulator (LBA) model of decision-making represents a choice as a race between two accumulators. The accumulators gather evidence until one of them reaches a threshold, triggering a decision response. The time taken to make the decision is the time taken to reach the threshold, plus a constant offset amount for processes unrelated to the decision. Variability arises from the starting point of the evidence accumulation process and its speed; both vary randomly from trial-to-trial and independently in each accumulator.

contributions for the two racing accumulators. The model parameters are constrained sensibly by the experimental conditions. For example, the thresholds are allowed to be different for speed-emphasis vs. accuracy-emphasis trials, but are constrained to be equal for all speed-emphasis trials.

The standard static model assumes that the data from different trials are independent, for each person, conditional on the parameters. The conditional density of all the observations is then

$$p\left(RT, RE | \tilde{b}, \tilde{A}, \tilde{v}^{(1)}, \tilde{v}^{(2)}, \tilde{\tau}\right) = \prod_{j=1}^S \prod_{i=1}^N \text{LBA}\left(RE_{ij}, RT_{ij} | \tilde{b}_j, \tilde{A}_j, \tilde{v}_j^{(1)}, \tilde{v}_j^{(2)}, \tilde{\tau}_j\right); \quad (1)$$

$S$  is the number of subjects,  $N$  is the number of decisions by each subject, and  $\text{LBA}()$  is the density function of the LBA model (see Brown & Heathcote, 2008; Terry et al., 2015).

We estimate  $\tilde{B}_j = \tilde{b}_j - \tilde{A}_j$  instead of directly estimating  $\tilde{b}_j$ , ensuring that the decision threshold is always larger than the starting point of evidence accumulation. We log-transform all parameters, so that  $B_j = \log(\tilde{B}_j)$ , etc. The log-transformed random effects are  $\alpha_j = \{B_j, A_j, v_j^{(1)}, v_j^{(2)}, \tau_j\}$ . An important advantage of log-transforming the model parameters is that it allows Gibbs sampling, if we take their joint distribution as multivariate normal, with mean  $\mu$  and covariance matrix  $\Sigma$ , that is:

$$\alpha_j | \mu, \Sigma \sim \mathcal{N}(\mu, \Sigma).$$

Gunawan et al. (2020) describe how the full covariance matrix  $\Sigma$  is estimated, which is advantageous when working with models such as the LBA where parameters tend to covary strongly.

**Three Time-Varying LBA Accounts.** Three extensions of the standard (static) LBA model that allow time-varying parameters for individual participants are considered. We call these the “AR”, “trend”, and “switching” models. The AR and trend models assume that the parameters for any participant in any given block of trials are constant, but that those parameters evolve over blocks. The two models differ in the prior that they assume for this evolution. The AR model assumes a first-order autoregressive prior and the trend model assumes a polynomial regression prior with linear and quadratic trends. The switching model is different from the other two in that it does not operate on blocks of trials, but at the level of individual trials. The switching model assumes that each person’s decision-making is governed by two separate vectors of random effects, representing two different mental states or two different modes or even “systems” for decision-making. These random effects are estimated from data and can differ in a wide variety of ways. For example, they could differ in the sensitivity of the decision-making process (drift rates), which might correspond to on-task vs. off-task states. Alternatively, they could differ in the speed-accuracy tradeoff parameters (thresholds or start points), which correspond to different strategies for balancing decision speed vs. caution. Switching between states is defined by a simple hidden Markov process. The transition matrix for the Markov process defines the probability on each trial of switching between states.

For the AR and trend models, we choose to examine the effects of time-on-task by splitting the data into blocks representing different time periods. While coarser and finer splits are possible in principle, we respect the designs of the original experiments by using blocks defined by their procedures. Using blocks to define time-on-task (instead of, e.g., single trials) is an important choice because it also allows the introduction of a significant theoretical advance – random effects for blocks. This allows us to relax an implausible assumption of previous work, that parameters did not have any error variability across blocks. That assumption has forced previous accounts of change with time-on-task to attribute all randomness to the static model. For example, suppose a participant generally improved over blocks, but also had one block of very poor performance near the end (perhaps due to fatigue, or mind-wandering). Our approach allows estimation of random effects for each block, for each subject. In the example above, this allows appropriate separation between the general improving trend and the outlying block with very different parameter settings. Previous time-on-task analyses would instead be forced to estimate a biased version of the general improvement parameters. A consequence of our approach is that time-on-task must be measured in blocks, and these blocks must be large enough to estimate random effects (our analyses use blocks between 20-100 trials each).

For the **autoregressive (AR)** process, for each subject,  $j = 1, \dots, S$ , and for each block,  $t = 1, \dots, T$ , the density of  $\alpha_{j,t}$  is

$$\alpha_{j,t} | \alpha_{j,t-1}, \phi, \mu, \Sigma \sim \mathcal{N}(\mu + \text{diag}(\phi)(\alpha_{j,t-1} - \mu), \Sigma), \quad (2)$$

$$\alpha_{j,1} | \mu, \Sigma \sim \mathcal{N}(\mu, \Sigma), \quad (3)$$

where  $\text{diag}(\phi)$  is the diagonal matrix with the diagonal vector of autoregressive coefficients  $\phi = (\phi_1, \dots, \phi_D)$ ;  $D$  is the dimension of  $\alpha_{j,t}$ , and for parsimony  $\phi$  is assumed to be the same

for all subjects ( $j$ ) and its elements are constrained to the interval  $(-1, 1)$  to ensure that distant time blocks are less correlated. Values of  $\phi$  near to 1 indicate a high correlation between adjacent blocks, while values of  $\phi$  near zero mean that the blocks are almost independent of each other. Equation (3) initializes the  $\alpha_{j,t}$  sequence by providing a prior distribution for the random effects in the first time period,  $\alpha_{j,1}$ ; the location of this prior distribution is  $\mu$  and its covariance matrix is  $\Sigma$ , that is, the group-level multivariate normal distribution. Our definition for the AR prior has useful properties for a psychological account of time-on-task. For example, it implies that the expected value (in the prior) of the random effects do not change with time. The expected correlations between random effects are approximately constant across blocks, and the correlations between the same random effect in different blocks falls away exponentially with the distance between the blocks.

The following priors are assumed for the group parameters in Equations (2) and (3):  $\mu \sim \mathcal{N}(0, I_D)$  and  $\Sigma \sim IW(v = 20, S_\alpha = I_D)$ ;  $IW$  denotes the inverse Wishart distribution. The inverse Wishart distribution is a standard prior assumption for covariance matrices, and is conjugate with the multivariate normal distribution; see e.g., Gelman et al. (2014). For the vector of autoregressive parameters, we assumed independent uniform priors,  $\phi_i \sim U(-1, 1)$  for  $i = 1, \dots, D$ .

For the **polynomial trend** model, for each subject  $j = 1, \dots, S$ , and for each time block,  $t = 1, \dots, T$ , the density of  $\alpha_{j,t}$  is

$$\alpha_{j,t} | \mu_t, \Sigma \sim \mathcal{N}(\mu_t, \Sigma); \quad (4)$$

the  $d^{th}$  component of  $\mu_t$  is  $\beta_{d1} + \beta_{d2}t + \beta_{d3}t^2$ ,  $d = 1, \dots, D$ . The polynomial coefficients have a standard normal distribution:  $\beta_{dk} \stackrel{i.i.d.}{\sim} N(0, 1)$ ,  $d = 1, \dots, D$ ,  $k = 1, 2, 3$  and the prior for  $\mu$  and  $\Sigma$  is the same as in the AR model.

The time-varying **Markov switching** model operates at the trial-by-trial level, rather than block-by-block, enabling it to also capture the micro-structure of decision-making. The switching model assumes that each participant has two different states in which they might perform the task<sup>1</sup>. These states are defined by different parameter settings for the evidence accumulation process; for example, one state may have a very fast setting for the drift rates, and the other state a very slow setting. The participant performs the decision-making task on any given trial in either one or the other of these states. The hidden Markov model describes the process by which the participant switches between states. On each trial, there is a fixed probability of switching from the current state to the other state. This probability can be different for switching in the different directions (i.e., a different probability for switching out of state 1 into state 2 than for switching out of state 2 into state 1), which allows the Markov transition matrix to be asymmetric. Psychologically, this is important as it allows for a non-uniform steady state distribution over states with one state more likely than the other.

It is psychologically plausible that the random effects for the two states are correlated – a participant who is faster than average in one state is also likely to be faster than average in the other state. To support this, we estimated a model in which the prior allowed for

<sup>1</sup>We limit our modelling to  $K = 2$  states, but note that the method extends naturally to any number of hidden states.

correlations in the random effects between states. Each participant’s performance was described by a vector of random effects,  $\alpha_j$ , which was twice the dimension as that for the other models, formed by concatenating the random effect vectors for the two states. For each participant, we also estimated two random effects for the switching probabilities. For subject  $j$ , we denote these by  $\xi_1$  and  $\xi_2$ , for the probabilities of switching out of states 1 and 2, respectively. Appendix C discusses estimation details for the Markov switching LBA model.

**Model Estimation.** The statistical difficulties associated with reliably estimating time-varying cognitive models have previously presented barriers to the theoretical progress with time-varying effects, including of practice, fatigue, and learning. In addition to the updated statistical modelling approaches outlined above, the methodology is made possible by our novel estimation methods, which build on recent developments in statistical treatments for the static LBA model (Gunawan et al., 2020). The estimation approaches use particle Metropolis within Gibbs (PMwG) to estimate the time-varying random effects models by defining an augmented parameter space which includes copies of all the model’s parameters, and the trajectories (history) of the particles representing these. This enables Metropolis-within-Gibbs sampling while guaranteeing that the samples are generated from the exact posterior.

We ran the PMwG algorithm with the number of particles fixed at  $R = 250$ . Three different sampling stages are employed; in the initial stage, the first 1,000 iterates are discarded as burn-in; the next 4,000 iterates are used in the adaptation stage to construct the efficient proposal densities for the random effects for the final sampling stage; finally, a total of 10,000 MCMC posterior draws are obtained in the sampling stage. For inference about the models’ performance, we extended the importance sampling based method of Tran et al. (in press), called IS<sup>2</sup>. This robustly and efficiently estimates the marginal likelihood of each dynamic model, thus supporting inference via Bayes factors. We ran the IS<sup>2</sup> algorithm with  $M = 10,000$  importance samples to estimate the log of the marginal likelihood. The number of particles used to obtain the unbiased estimate of the likelihood was set to  $R = 500$ , and the Monte Carlo standard errors of the log of the marginal likelihood estimate were obtained by bootstrapping the importance samples. The details of the estimation methods are given in Appendix B for the AR and trend models, and in Appendix C for the Markov switching model. These appendices include statistical properties related to our new algorithms and practical computational details. The code to implement all the algorithms is available from [osf.io/x29wb](https://osf.io/x29wb). That site also has supplementary material which demonstrates the statistical robustness of the methods, including a simulation study showing that our methods appropriately recover the data-generating process and data-generating parameters of the models.

## Data

### Dynamic Effects in Perceptual Decision-Making

Forstmann et al. (2008) had 19 participants make repeated decisions about the direction of motion shown in a random dot kinematogram. We analyzed data from the behavioral training, pre-scanning, session in which each participant made 840 decisions distributed evenly over three conditions. These conditions changed the instructions given to

participants about whether they should emphasize the speed of their decisions, the accuracy of their decisions, or adopt a “neutral” balance between speed-emphasis and accuracy-emphasis. The data reveal large changes in both the speed (response time) and accuracy of decisions between speed-emphasis and accuracy-emphasis conditions, but only small differences between the accuracy-emphasis and neutral-emphasis conditions. Full details of the method are on p.17541 of the original article.

To model the decisions in these data, we follow the same LBA specification as in the original article. The modelling collapses across left- and right-moving stimuli, forcing the same mean drift rate for the accumulator corresponding to a “right” response to a right-moving stimulus as for the accumulator corresponding to a “left” response to a left-moving stimulus; let  $v^{(c)}$  be this mean drift rate. Similarly, drift rates for the accumulators corresponding to the wrong direction of motion are constrained to be equal and denoted by  $v^{(e)}$ . Three different response thresholds are estimated, for the speed, neutral, and accuracy conditions:  $B^{(s)}$ ,  $B^{(n)}$ , and  $B^{(a)}$  respectively. Two other parameters are estimated: the time taken by non-decision process ( $\tau$ ) and the width of the uniform distribution for start points in evidence accumulation ( $A$ ). To investigate time-on-task, we divided the trials into blocks matching the experimental procedure, of size  $n = 50$  trials on average (there is some variability due to a few missing data). There are  $T = 17$  blocks for each subject.

### Dynamic Effects in Lexical Decision-Making – Block-by-Block Speed Accuracy Tradeoff

The participants in Experiment 1 of Wagenmakers et al. (2008) made decisions about whether letter strings are valid English words (e.g., “RACE”) or non-words (e.g., “RAXE”). Each of 17 participants made decisions about 1,920 letter strings. Half of the letter strings are non-words. The other half are divided across three types of words: high frequency words which are very common in written English (e.g., “ROAD”); low frequency words which are uncommon (e.g., “RITE”); and very low frequency words, which are extremely rare (e.g., “RAME”) Decisions are arranged into  $T = 20$  blocks of  $n = 96$  decisions (trials) each. The instructions given to participants change from block-to-block; in alternate blocks, participants are instructed to emphasize the accuracy or the speed of their decisions. Full details of the method are on p.144 of the original article. We use the experimenter-defined blocks to investigate the effects of time-on-task:  $n = 96$  trials in each of  $T = 20$  blocks, except for a very small number of missing trials for some participants.

To describe the lexical decisions with the LBA model, we assume that: (a) the speed-emphasis vs. accuracy-emphasis manipulation influences only threshold settings; and (b) the different stimulus categories (word frequency) influences only the means of the drift rate distributions. These are sometimes called “selective influence” assumptions, and are important for the psychological interpretation of the theory (Ratcliff & Rouder, 1998; Voss, Rothermund, & Voss, 2004). These assumptions result in the following random effects for participant  $j$  in block  $t$ ,

$$\left( B_{j,t}^{(s)}, B_{j,t}^{(a)}, A_{j,t}, v_{j,t}^{(hf,W)}, v_{j,t}^{(lf,W)}, v_{j,t}^{(vlf,W)}, v_{j,t}^{(nw,W)}, v_{j,t}^{(hf,NW)}, v_{j,t}^{(lf,NW)}, v_{j,t}^{(vlf,NW)}, v_{j,t}^{(nw,NW)}, \tau_{j,t} \right), \quad (5)$$

such that independent mean drift rates ( $v$ ) are estimated for each stimulus class ( $hf$ ,  $lf$ ,  $vlf$ ,  $nw$ ) and response ( $W$ ,  $NW$ ).

### Dynamic Effects in Lexical Decision-Making – Effects of Base Rate

Experiment 2 of Wagenmakers et al. (2008) is very similar to Experiment 1, except with 19 new participants. The 1,920 trials were split into alternating blocks of 96 trials each. The blocks are either dominated by words or non-words: in some blocks there are 24 words and 72 non-words, and in the other blocks there are 72 words and 24 non-words. Blocks alternated between non-word-dominated and word-dominated. Before each block begins, participants are reminded which kind of stimulus string will be most common in the upcoming block of trials. Full details of the method are on p.152 of the original article. We again use the experimenter-defined blocks to investigate the effects of time-on-task ( $n = 96$  and  $T = 20$ ).

To describe the lexical decisions in this experiment, we allow for response bias, expressed as different decision thresholds in the accumulators corresponding to “word” ( $B^{(\cdot, W)}$ ) and “non-word” ( $B^{(\cdot, NW)}$ ) responses. These are allowed to be different between the blocks dominated by word ( $B^{(w, \cdot)}$ ) and non-word ( $B^{(nw, \cdot)}$ ) stimuli, following the hypothesis that the base rate of the stimulus classes should influence participants’ biases. These assumptions result in the following random effects for participant  $j$  in block  $t$ ,

$$\left( B_{j,t}^{(w,W)}, B_{j,t}^{(w,NW)}, B_{j,t}^{(nw,W)}, B_{j,t}^{(nw,NW)}, A_{j,t}, v_{j,t}^{(hf,W)}, v_{j,t}^{(lf,W)}, v_{j,t}^{(vlf,W)}, v_{j,t}^{(nw,W)}, v_{j,t}^{(hf,NW)}, v_{j,t}^{(lf,NW)}, v_{j,t}^{(vlf,NW)}, v_{j,t}^{(nw,NW)}, \tau_{j,t} \right). \quad (6)$$

## Results

### Model Performance

Table 1 shows that, for all three experiments, the Markov switching model provided the best explanation of the data. The differences between the marginal likelihoods for the models are large compared to the scales usually used for such comparisons; e.g., they correspond to Bayes factors much larger than  $10^6$  for all pairwise comparisons. The Monte-Carlo errors of the log of the estimated marginal likelihoods (in brackets) are small, confirming the practical efficiency of the method. For all experiments, the auto-regressive (AR) model has the second-best marginal likelihood. The time-varying models provide a much better explanation of the data than the standard static LBA. The static model provides a poorer account than all three time-varying models in almost every case; the only exception is that the static model out-performs the polynomial trend model in the data from Forstmann et al. (2008).

To examine goodness of fit, we compare posterior predictive data generated from the Markov switching model against the observed data using the proportion of correct responses and the mean RT. Figure 3 shows these comparisons broken down by time-on-task (trials – smoothed) and by the important experimental conditions, but averaged across participants. The Markov switching model captures the fundamental patterns in the data. Changes in threshold settings capture the differences in RT between urgency conditions well. The much

Table 1

*Model selection results for data from the three experiments: logs of the estimated marginal likelihoods and bootstrap-estimated standard errors (in brackets). Bold font shows the model with the largest estimated marginal likelihood for each data set. For all three experiments, the preferred model was the Markov switching model.*

	<i>Static</i>	<i>AR</i>	<i>Trend</i>	<i>Switching</i>
Forstmann et al. (2008)	7458.77 (0.05)	7888.98 (0.12)	7417.03 (0.16)	<b>8198.70</b> (3.31)
Wagenmakers et al. (2008) Exp. 1	5970.06 (0.17)	8184.68 (0.18)	8003.11 (0.53)	<b>8305.11</b> (2.86)
Wagenmakers et al. (2008) Exp. 2	9629.81 (0.35)	10323.75 (0.75)	9914.80 (0.46)	<b>11292.49</b> (3.86)

smaller changes in accuracy between urgency conditions are slightly less well captured. The Markov switching model is quite tightly constrained in the way it can accommodate time-on-task effects. The model predicts those changes by predicting changes in the proportion of time spent in the two hidden states. This requires the model to predict matching changes in both accuracy and RT. For the most part, this is also observed in data, e.g., the declining accuracy and RT for Experiment 1 of Wagenmakers et al. (2008), but not always, e.g., the first phase of Forstmann et al.’s 2008 experiment has rapidly decreasing accuracy along with increasing RT. Of note, the model under-predicts average accuracy in the easiest conditions of Wagenmakers et al.’s experiments – those conditions where observed accuracy was near ceiling. This limitation is imposed by the tightly constrained parameterization of the basic decision-making model in each state. That parameterization is also the same as used for the static model, which shows the same under-prediction of the high-accuracy observations, and was chosen to match previous investigations of these data.

In addition to providing a good fit at the level of averaged data, the Markov switching model also provides a good fit to individual subjects’ data, at least for most participants. We generated plots similar to Figure 3 but separately for every individual participant. Figure 4 shows just one of six such plots; the fit to the RT data from Wagenmakers et al. (2008). Appendix A contains the other five plots: accuracy fit for Wagenmakers et al.’s Experiment 1 data, and both accuracy and RT fits for Wagenmakers et al.’s Experiment 2 data and Forstmann et al.’s data. Figure 4 shows that effects apparent in the group averaged fits are borne out in individual fits. The Markov switching model captures changes between conditions and changes with time-on-task for most individual participants.

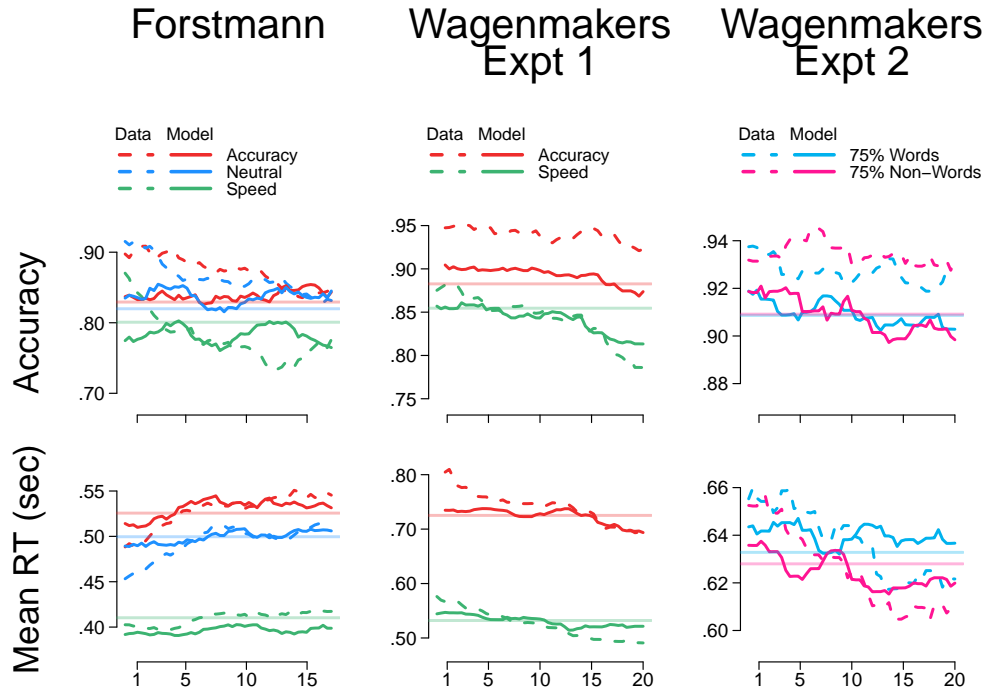


*Figure 3.* Data (dashed lines) from experiments reported by Forstmann et al. (2008) and Wagenmakers et al. (2008), shown in columns. The rows show how average accuracy and average RT change with time-on-task ( $x$ -axis, with kernel smoothing). Posterior predictive data from the Markov switching model are overlaid as solid lines, and from the static model as transparent lines.

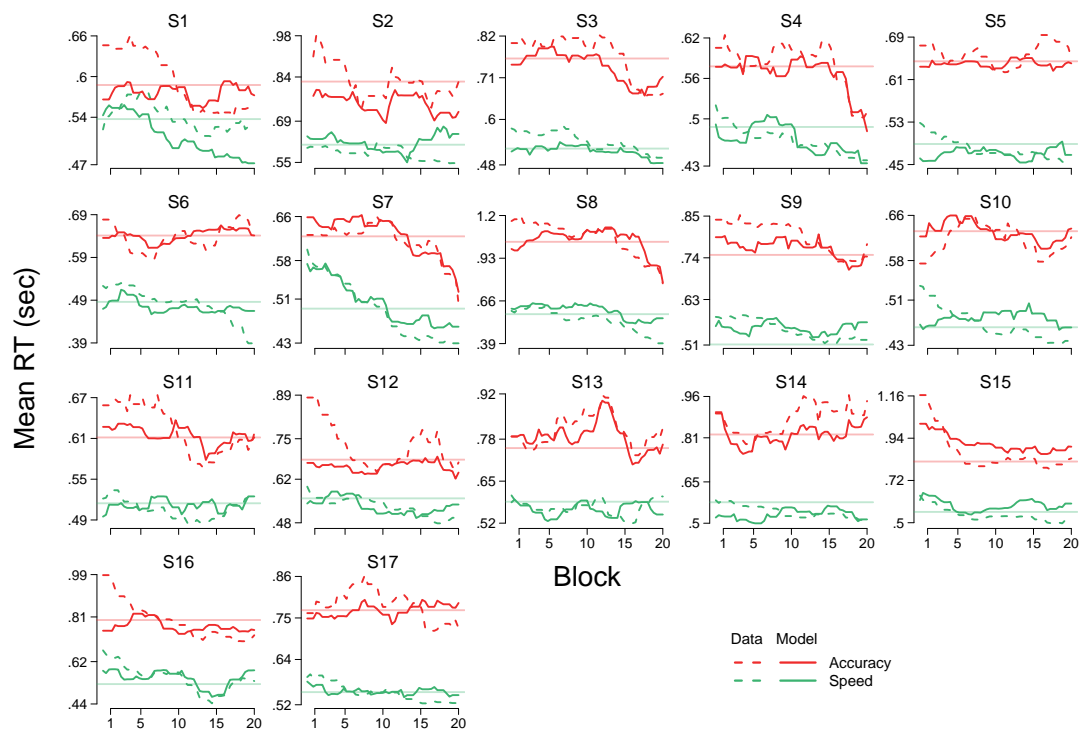


*Figure 4.* Mean RT (dashed lines) and model fit (solid lines for the Markov switching model; straight transparent lines for the static model) for Experiment 1 in Wagenmakers et al. (2008). Each panel shows a different participant. The red and green lines show performance in the accuracy and speed emphasis conditions, across time-on-task.

Table 2

Group-level posterior parameter estimates for the two states of the Markov switching model, for each of the three experiments. Corresponding estimates for the static LBA model are also shown (in brackets) for comparison. Parameters are grouped by psychological processes: Caution ( $b - \frac{A}{2}$ ); non-decision time ( $\tau$ ); and drift rate ( $v$ ). For drift rates in both of Wagenmakers et al.’s experiments the bracketed labels indicate the response accumulator (“W” for “word” response and “NW” for “nonword” response) and stimulus condition (“hf”, “lf”, “vlf” respectively for high frequency, low frequency and very low frequency words, and “nw” for nonwords). Statistically reliable differences between state 1 vs. state 2 are indicated by bold face. These correspond to less than 2.5% overlap between posterior distributions across states.

	Forstmann	Wagenmakers Exp. 1						Wagenmakers Exp. 2					
	State	1	2	(Static)		1	2	(Static)		1	2	(Static)	
Caution	Accuracy	<b>0.74</b>	<b>0.92</b>	(0.98)	Accuracy	<b>0.98</b>	<b>1.21</b>	(1.37)	(w,W)	<b>0.53</b>	<b>0.83</b>	(0.96)	
	Neutral	<b>0.68</b>	<b>0.85</b>	(0.91)	Speed	<b>0.57</b>	<b>0.75</b>	(0.85)	(w,NW)	<b>0.91</b>	<b>1.22</b>	(1.39)	
	Speed	<b>0.46</b>	<b>0.56</b>	(0.63)					(nw,W)	<b>0.85</b>	<b>1.14</b>	(1.30)	
									(nw,NW)	<b>0.54</b>	<b>0.84</b>	(0.96)	
$\tau$		0.23	0.21	(0.18)		0.29	0.20	(0.15)		0.29	0.23	(0.18)	
Drift Rate	Correct	1.16	1.32	(1.40)	(hf,W)	3.39	3.37	(3.65)	(hf,W)	3.27	3.28	(3.47)	
	Incorrect	3.06	3.15	(3.09)	(lf,W)	2.71	2.71	(3.01)	(lf,W)	2.55	2.71	(2.87)	
					(vlf,W)	2.34	2.41	(2.64)	(vlf,W)	2.13	2.35	(2.51)	
					(nw,W)	<b>0.37</b>	<b>0.77</b>	(0.67)	(nw,W)	0.21	0.22	(0.52)	
					(hf,NW)	<b>0.58</b>	<b>1.07</b>	(0.85)	(hf,NW)	0.44	0.42	(0.64)	
					(lf,NW)	<b>0.68</b>	<b>1.26</b>	(1.15)	(lf,NW)	0.67	0.55	(0.93)	
					(vlf,NW)	<b>1.07</b>	<b>1.57</b>	(1.48)	(vlf,NW)	1.13	0.94	(1.31)	
					(nw,NW)	2.69	2.67	(2.96)	(nw,NW)	2.60	2.66	(2.86)	

### Psychological Interpretation of the Markov Switching Model

Table 2 reports the mean posterior estimates for the Markov switching model’s parameters, for both hidden states and all three experiments. For the experiment reported by Forstmann et al. (2008), and Experiment 2 of Wagenmakers et al. (2008), the model has identified two states which differ *only* in the level of decision caution. For those experiments, the drift rate and non-decision time parameters are not reliably different between states; the posterior distributions for the difference between states includes zero for all those parameters. However, in both experiments, participants adopt a more cautious speed-accuracy trade-off strategy in State #2 than State #1. It is common to operationalize decision caution as the average amount of evidence that must be accumulated to reach the decision threshold (Forstmann et al., 2008; Rae, Heathcote, Donkin, Averell, & Brown, 2014), which is  $b - \frac{A}{2}$ . For the three conditions in Forstmann et al.’s experiment, caution is reliably larger in State #2 than State #1, as indicated by the 95% credible intervals for the difference in caution between states, which excluded zero in all three conditions: accuracy (0.06, 0.32); neutral (0.06, 0.29); speed (0.03, 0.19). For each of the four threshold estimates in Wagenmakers et al.’s Experiment 2, caution is reliably higher in State #2 than State #1:  $w, W = (.15, .44)$ ;  $w, NW = (.11, .50)$ ;  $nw, W = (.12, .48)$ ;  $nw, NW = (.15, .44)$ . This is also true for the two estimates in Wagenmakers et al.’s Experiment 1: accuracy (.05, .42); speed (.07, .31).

The Markov switching model leads to different psychological interpretations for Experiment 1 of Wagenmakers et al. (2008). From those data, the model identified hidden states which differed in both the level of caution adopted and the level of response inhibition engaged by the decision-maker. As for the other experiments, State #1 implied more urgent decision-making than State #2 – less distance from start of evidence accumulation to threshold, on average. In addition, drift rate differences between states implied changes in the rate of evidence accumulation which are psychologically meaningful. The speed of evidence accumulation, i.e., drift rate, for accumulators which correspond to *correct* response choices did *not* differ between states. These are drift rates for the accumulator corresponding to the “nonword” response, for those trials when the stimulus is a nonword – parameter “nw,NW” in Table 2 – and the drift rates for the accumulator corresponding to the “word” response for trials when the stimulus is a word of any frequency – parameters “hf,W”, “lf,W”, and “vlf,W” in Table 2. Instead, the differences between states were confined solely to the rate at which evidence accumulated for *wrong* responses: drift rates for the “word” accumulator during nonword trials, and the “nonword” accumulator during word trials; parameters “hf,NW”, “lf,NW”, “vlf,NW”, and “nw,W” in Table 2. Since these parameters represent the rate of accumulation of evidence in favor of incorrect responses, higher values indicate poorer performance. In State #2, the drift rates for incorrect choices were larger by between 0.40 and 0.59 units than in State #1. These differences between states were statistically significant, posterior distributions for the differences have 95% intervals excluding zero:  $nw, W = (.11, .73)$ ;  $hf, NW = (.10, .91)$ ;  $lf, NW = (.17, 1.01)$ ;  $vlf, NW = (.08, .94)$ . To put the magnitude of the differences in context, the difference between the drift rates for the two accumulators in State #1 was about 1.27 in the most difficult condition, with very low frequency word stimuli. This implies that between 30% and 45% of the participants’ sensitivity to the core decision task was lost in State #2. The

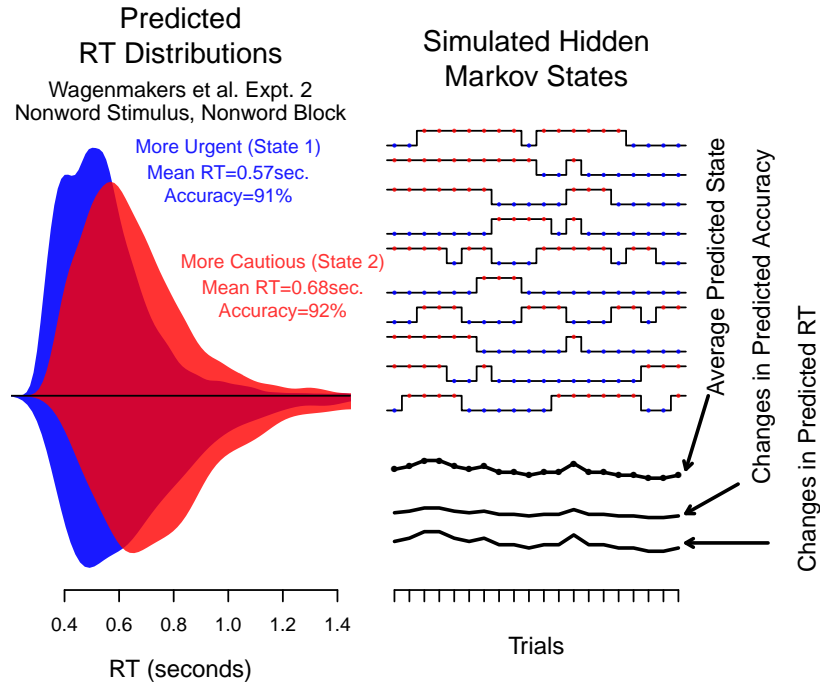
psychological implication of our analyses of Experiment 1 of Wagenmakers et al. (2008) is that participants switched between two cognitive states during performance. In one of those states, participants were much less effective at appropriately suppressing incorrect responses. This represents a weakening of executive functions related to inhibitory control (Karayanidis et al., 2009; Monsell, 2003; Monsell & Mizon, 2006).

Table 2 also shows, in brackets, parameter estimates from static LBA fits to the three data sets. Naively, one might expect that parameters estimated from the static model might fall mid-way between the parameters estimated for the two hidden states of the Markov switching model. Comparison of the values in Table 2 shows that this is not the case. Instead, it appears that the standard approach of fitting a static model to data which are more complex introduces estimation bias. The estimated time taken by non-decision process (parameter  $\tau$ ) is substantially smaller for the static model than for either state in Markov switching model, in all three experiments. Given existing knowledge about the speed of simple detection tasks (e.g., Luce, 1986) it seems likely that the slower estimates – from the Markov switching model – are closer to correct than the faster estimates from the static model. Similarly, estimated caution levels are larger from the static model than from the Markov switching model, in every condition, for all three experiments. For the most part, drift rate estimates are larger for the static model than for the Markov switching model, although there are exceptions in a small number of conditions (drift rates for the accumulator corresponding to the incorrect response, in Experiment 1 of Wagenmakers et al., 2008).

### Longer-Term Dynamics

Figure 5 illustrates the Markov switching model in detail, using the actual (group mean posterior) parameter estimates from Experiment 2 of Wagenmakers et al. (2008). The left panel shows the predicted response time and accuracy from State #1 vs #2, using different colors. The RT distributions above and below the horizontal centre line show predictions for correct and incorrect responses, respectively. Predictions for the observed data arise from mixtures of responses generated from the two states. The mixing is governed by the hidden Markov process illustrated in the right-hand half of the figure. There, the stepped lines with colored dots indicate sample trajectories of the Markov process, showing how the internal state switches randomly every few trials. The solid lines below the stepped traces illustrate how changes in state can lead, on average, to time-varying effects as observed in the data.

Although the Markov process assumed a stationary prior, the time-on-task effects are captured by changes in the posterior distribution of state probabilities. Figure 5 also illustrates this process. The three solid lines below the sample trajectories (stepped lines) show the how the average time spent in each state (averaged across sample trajectories) changes, and how this subsequently changes the predicted mean RT and accuracy. Figure 6 shows these effects as changes in the probability of being in State #1 over blocks, as well as the between-participant variability in state probabilities. Performance in Forstmann et al.’s study initially shows a slight decrease in the probability of being in the less cautious State #1, followed by a long period of stable performance, with approximately half of the data generated from each state. Time-on-task effects are larger in the two experiments reported by Wagenmakers et al.. In both cases, the model reveals an increasing tendency



*Figure 5.* Illustration of the Markov switching model, using estimates from Experiment 2 of Wagenmakers et al. (2008). The left panel shows the predicted RT distributions corresponding to the two states (different colours). These predictions are generated using the mean group-level posterior parameters, for one example condition (a non-word stimulus presented during a block with 75% non-words). Distributions of correct and incorrect choices are shown above and below the horizontal axes, respectively. The two states correspond to more cautious vs. more urgent decision-making, leading to changes in RT but negligible effects on accuracy. The right panel shows posterior samples from the Markov process, switching between states (stepped lines with colored dots). The three solid lines below show the corresponding average predictions for the probability of being in each state, and subsequent accuracy and mean RT.

for participants to adopt less thorough decision-making approaches over time, but with different psychological causes in the two experiments. For Wagenmakers et al.'s Experiment 1 (middle panel), the model identifies two states which differ in how engaged the participants are. The probability of adopting the more engaged decision-making State #1 decreases rapidly over the first three blocks, and continues to decline slowly thereafter. This reflects decreasing levels of both caution and inhibitory control over the course of the experiment. In Experiment 2 (lower panel), the model identifies an increasing reliance on State #1 over blocks, corresponding to less cautious decision-making. In the first few blocks, the lower-caution State #1 generates around one third of the data, but this flipped such that in the final few blocks that state generates nearly 60% of the data.

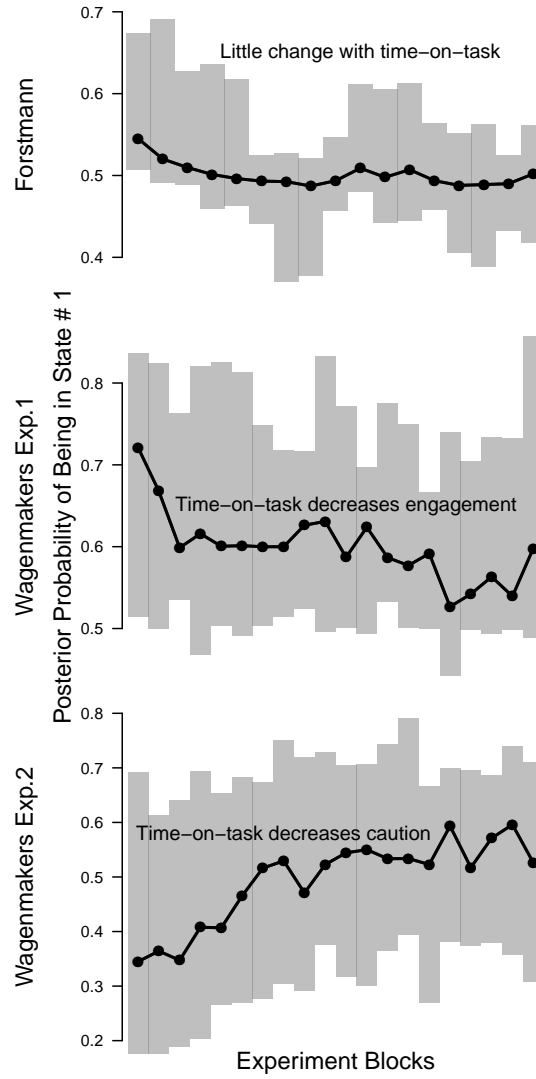


*Figure 6.* Time-on-task effects are captured by the Markov switching model via changes in the posterior probability of the states. Over blocks of the experiments ( $x$ -axes), the posterior probability of decisions arising from State #1 changes. The solid lines with dots show the median, across participants, of this posterior probability. The shaded rectangles indicate between-subject variability, by showing the inter-quartile range for each block. For the two experiments reported by Wagenmakers et al. (2008), these results are consistent with a steady decrease in the care taken by participants over time: for Experiment 1, this was caused by decreasing use of the more-engaged State #1; for Experiment 2, this was caused by increasing use of the less-cautious State #1. For the experiment of Forstmann et al. (2008), there is an initial small change followed by a long period of stable performance.

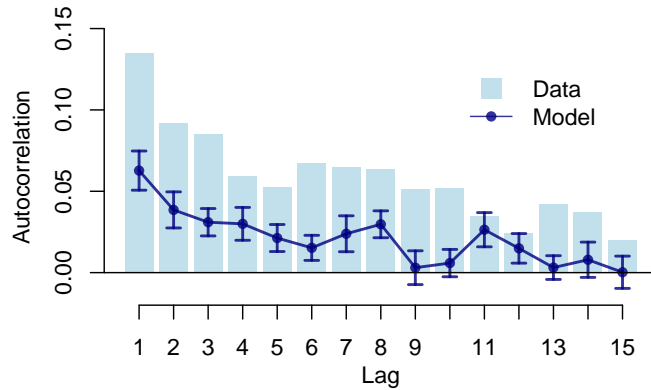


Figure 7. Autocorrelation of response times in data from Forstmann et al. (2008). Light blue bars show autocorrelation functions from data averaged over subjects. Dark blue lines show the same from posterior predictive data generated by the Markov switching model (error bars show posterior standard deviations).

### Shorter-Term Dynamics

A ubiquitous feature of decision-making data – indeed, behavioral data from many paradigms – is correlation between successive observations. In response time data, this is often observed in autocorrelation functions which persist across several, or even dozens, of trials (e.g., Brown et al., 2008; Stewart, Brown, & Chater, 2005; Stewart & Matthews, 2009; Vickers & Lee, 1998, 2000). These autocorrelations are also observed in the data we investigated: Figure 7 shows the autocorrelation function for the data from Forstmann et al. (2008), with persistent correlation between response times on decisions up to 15 trials apart (bars). An interesting consequence of the Markov switching model is its potential to provide a psychological explanation for the process which produces autocorrelation. Under the Markov switching model, nearby trials are more likely to be produced from the same hidden state than trials far apart in time, because every intervening trial adds another chance for a change in hidden state, leading to changed behavioral predictions. Figure 7 demonstrates that the Markov switching model reproduces the basic qualitative properties of autocorrelation in the data (dark blue line). This result is more impressive because the model was not constructed with the goal of explaining microstructure such as autocorrelation – the autocorrelation is a natural consequence of the model structure. This is in contrast, for example, to theories such as SAMBA (Brown et al., 2008) and PAGAN (Vickers & Lee, 1998) which “build in” autocorrelation via complicated additional mechanisms. The Markov switching model tends to underestimate the magnitude of autocorrelation, at most lags. One interpretation of this underprediction is that the Markov switching model provides an explanation for one source of autocorrelation in the data, but not all sources.

### Discussion

Human behavior is fundamentally dynamic. The improvements gained through repeated practice are often large, and are reliably observed across a wide range of behavior, from very simple counting tasks to complex tasks with multiple stages (Evans et al., 2018;

A. Newell & Rosenbloom, 1981; Wynton & Anglim, 2017). In other cases, time-on-task leads to steady decreases in performance, via fatigue (Dorrian, Roach, Fletcher, & Dawson, 2007; Van der Linden, Frese, & Meijman, 2003); and yet, in other cases, to changing periods of good and bad performance, caused by poor cognitive control and “mind-wandering” (also called “task unrelated thoughts”: Giambra, 1995; Mittner et al., 2016). In some cases, cognitive changes with time-on-task are a central focus of the research activity, and are directly investigated.

However, changes with time-on-task are often ignored. When off-the-shelf analysis tools such as ANOVA are applied, the data are routinely aggregated across time-on-task. More importantly, the same approximation is usually made even when more meaningful psychological theories are applied. There are dozens, or perhaps hundreds, of model-based analyses of the cognitive processes underlying simple decision-making using evidence accumulation models similar to the one used above. These include applied studies which reveal how experimental manipulations or person-based variables are associated with differences in decision-making due to changed caution, sensitivity, or other model parameters, while other studies focus on developing or elaborating the decision-making theories themselves, including extension; see Ratcliff et al. (2016) for a review. However, in almost all cases, the data are treated as if repeated decisions are unchanging and independent.

Our work provides an approach for resolving the obvious discrepancies between the reliably observed effects of time-on-task and the psychological theories which mostly ignore them. We extend a standard static model of decision-making, the linear ballistic accumulator, in psychologically-meaningful ways to account for time-varying behaviour. We explore extensions in which the model’s parameters evolve with time on task. The most successful extension is a Markov switching model which allows for decision-making behavior to be generated from one of two latent states, with different parameters. Behaviour switches between states according to a hidden Markov process, which represents a plausible process-level theory for the evolution of psychological states (see also: Busemeyer, Wang, & Lambert-Mogiliansky, 2009; Hamaker, Grasman, & Kamphuis, 2010; Visser, Raijmakers, & van der Maas, 2009).

### **Different Approaches to Time-Varying Effects**

Some earlier work takes into account time-varying effects in data, but our approach differs in critical ways. For example, the PAGAN model of Vickers and Lee (1998) and the SAMBA model of Brown et al. (2008) extend evidence accumulation models to cover some time-varying effects. These models are based on accumulators racing to make decisions, but with elaborated elements describing how the properties of the accumulators change from decision-to-decision; e.g., due to meta-cognitive changes in confidence, or to facilitate repeated responses. These models are very interesting and have had substantial success in expanding understanding in their respective fields. However, incorporating time-varying effects incurs a substantial cost – those models are intractable, and cannot be meaningfully estimated from the data. Their authors demonstrate that the models reproduce important patterns in the data with hand-tuned parameter settings, but this is very different from our approach. Our time-varying models allow accurate estimation of parameters from data. This puts them in the class of models that are used for “cognitive psychometrics”, drawing psychologically-meaningful inferences from data by comparing model estimates between

conditions and groups. Other work has extended reinforcement learning models to incorporate evidence accumulation processes. Most successful in this regard are the combinations of reinforcement learning models and diffusion models (RL-diffusion: Pedersen & Frank, 2020; Pedersen, Frank, & Biele, 2017; Wiecki, Sofer, & Frank, 2013). These models describe how the drift rate of a diffusion model can be linked to the output of a reinforcement learning model. The resultant combination can capture time-varying effects in experiments where those effects occur due to value learning or reinforcement and reward. The more general application of RL-diffusion is limited by both scientific considerations related to changes caused by any effects other than reinforcement learning, and statistical considerations. For example, the three data sets analyzed above all include within-subject manipulations (like almost all psychological experiments) and time-varying effects not caused by reinforcement. Both of these are not easy to manage in the RL-diffusion framework developed of Pedersen and Frank.

Other earlier investigations of time-varying effects make an opposite compromise, by replacing detailed psychological models of the basic psychological process with simplified, descriptive, accounts. For example, Craigmile et al. (2010) makes detailed studies of time varying effects in RT data, and develops correspondingly sophisticated model estimation methods; see also Peruggia, Van Zandt, and Chen (2002). These authors treat the decision-making process descriptively, for example using a Weibull distribution for response times, which limits the inferences that can be drawn about psychological processing. In related work, Turner, Van Zandt, and Brown (2011) model time-varying effects in recognition, but assume a simplified, descriptive account of the basic processes (signal detection theory). Our approach is an important advance that uses a psychological process model of the underlying phenomenon, like Vickers and Lee (1998) and Brown et al. (2008), but it also supports accurate parameter estimation, and practical use, similarly to Craigmile et al. (2010) and Peruggia et al. (2002).

## Future Directions and Conclusions

Of the three accounts we investigate for time-varying effects, only the Markov switching model represents a psychologically meaningful process-level explanation (for review, see Visser, 2011). This makes it heartening that the Markov switching model is also preferred by statistical model selection with marginal likelihood. The switching model adopts the plausible assumption that observed behavior is actually a mixture over states; we assume two states, but this is not a strong commitment. The mixing process itself is further explained by a hidden Markov process: behavior is always generated from just one of the two states, and at each moment there is a fixed probability of switching into the other state. This theory entails interesting links to research on “Type 1” vs. “Type 2” decision-making (B. R. Newell & Shanks, 2014) as well as mind-wandering (Mittner et al., 2014, 2016).

Our models and estimation methods may be useful in future applications to decision-making data. One way to use them is to screen data for the presence of important time-on-task effects. Identifying these effects is usually harder than plotting the data, because the effects can disappear in averages, and be nonlinear in individuals. Model comparison between the static and time-varying versions of the LBA can reveal the presence of time-varying effects. Analysis of the parameter estimates can help to interpret the nature of time-on-task effects, and identify the underlying psychological causes. Our modelling ap-

proach is likely to be useful beyond the specific application to the LBA model, and beyond decision-making research more generally. The central idea involves incorporating statistically tractable models for time series as descriptions of the changes in model parameters for individual subjects with time-on-task. This approach presents some estimation challenges, which are surmountable for many psychological theories, given recent advances in statistical and computational approaches. We hope that our approach is used in two ways: as a way to routinely model time-on-task effects in simple decision-making; and, more generally, to extend quantitative theories of cognition to investigate interesting effects such as those of practice, learning, and fatigue.

## References

- Andrieu, C., Doucet, A., & Holenstein, R. (2010). Particle Markov chain Monte Carlo methods. *Journal of the Royal Statistical Society, Series B*, 72, 1-33.
- Brown, S. D., & Heathcote, A. (2008). The simplest complete model of choice response time: Linear ballistic accumulation. *Cognitive psychology*, 57(3), 153-178.
- Brown, S. D., Marley, A. A. J., Donkin, C., & Heathcote, A. (2008). An integrated model of choices and response times in absolute identification. *Psychological Review*, 115, 396-425.
- Bunch, P., Lindsten, F., & Singh, S. S. (2015). Particle Gibbs with refreshed backward simulation. *IEEE International conference on acoustics, speech, and signal processing*.
- Bussemeyer, J. R., Wang, Z., & Lambert-Mogiliansky, A. (2009). Empirical comparison of markov and quantum models of decision making. *Journal of Mathematical Psychology*, 53(5), 423-433.
- Chib, S., & Jeliazkov, I. (2001). Marginal likelihood from the Metropolis-Hastings output. *Journal of American Statistical Association*, 96(453), 270-281.
- Christoff, K., Irving, Z. C., Fox, K. C. R., Spreng, R. N., & Andrews-Hanna, J. R. (2016). Mind-wandering as spontaneous thought: A dynamic framework. *Nature Reviews Neuroscience*, 17, 718-731.
- Craigmile, P. F., Peruggia, M., & Van Zandt, T. (2010). An autocorrelated mixture model for sequences of response time data. *Psychometrika*, 75, 613-632.
- Donkin, C., & Brown, S. D. (2018). Response times and decision-making. *Stevens' Handbook of Experimental Psychology and Cognitive Neuroscience, Methodology*, 349.
- Donkin, C., Brown, S. D., & Heathcote, A. (2009). The overconstraint of response time models: Rethinking the scaling problem. *Psychonomic Bulletin & Review*, 16(6), 1129-1135.
- Dorrian, J., Roach, G. D., Fletcher, A., & Dawson, D. (2007). Simulated train driving: fatigue, self-awareness and cognitive disengagement. *Applied ergonomics*, 38(2), 155-166.
- Evans, N. J., Brown, S. D., Mewhort, D. J., & Heathcote, A. (2018). Refining the law of practice. *Psychological review*, 125(4), 592.
- Evans, N. J., & Hawkins, G. E. (2019). When humans behave like monkeys: Feedback delays and extensive practice increase the efficiency of speeded decisions. *Cognition*, 184, 11-18.
- Forstmann, B. U., Dutilh, G., Brown, S., Neumann, J., Von Cramon, D. Y., Ridderinkhof, K. R., & Wagenmakers, E.-J. (2008). Striatum and pre-sma facilitate decision-making under time pressure. *Proceedings of the National Academy of Sciences*, 105(45), 17538-17542.
- Gelman, A., Carlin, J. B., Stern, H. S., Dunson, D. B., Vehtari, A., & Rubin, D. B. (2014). *Bayesian Data Analysis* (3rd ed.). CRC Press.
- Giambra, L. M. (1995). A laboratory method for investigating influences on switching attention to task-unrelated imagery and thought. *Consciousness and Cognition*, 4, 1-21.
- Gunawan, D., Carter, C., Fiebig, D. G., & Kohn, R. (2017). Efficient Bayesian estimation for flexible panel models for multivariate outcomes: impact of life events on mental health and excessive alcohol consumption. *arXiv preprint arXiv:1706.03953v1*.
- Gunawan, D., Hawkins, G. E., Tran, M.-N., Kohn, R., & Brown, S. (2020). New estimation approaches for the hierarchical linear ballistic accumulator model. *Journal of Mathematical Psychology*, 96, 102368.
- Hamaker, E. L., Grasman, R. P., & Kamphuis, J. H. (2010). Regime-switching models to study psychological processes. In *Individual pathways of change: Statistical models for analyzing learning and development* (p. 155-168). American Psychological Association.
- Heathcote, A., Brown, S., & Mewhort, D. J. K. (2000). The power law repealed: The case for an exponential law of practice. *Psychonomic Bulletin & Review*, 7, 185-207.
- Hesterberg, T. (1995). Weighted average importance sampling and defensive mixture distributions. *Technometrics*, 37, 185-194.
- Karayanidis, F., Mansfield, E. L., Galloway, K. L., Smith, J. L., Provost, A., & Heathcote, A. J.

- (2009). Anticipatory reconfiguration elicited by fully and partially informative cues that validly predict a switch in task. *Cognitive, Affective, & Behavioral Neuroscience*, 9, 202–215.
- Kim, S., Potter, K., Craigmile, P. F., Peruggia, M., & Van Zandt, T. (2017). A Bayesian race model for recognition memory. *Journal of the American Statistical Association*, 112(517), 77–91.
- Luce, R. D. (1986). *Response times*. New York: Oxford University Press.
- McVay, J. C., & Kane, M. J. (2010). Does mind wandering reflect executive function or executive failure? Comment on Smallwood and Schooler (2006) and Watkins (2008). *Psychological Bulletin*, 136, 188–207.
- Mittner, M., Boekel, W., Tucker, A. M., Turner, B. M., Heathcote, A., & Forstmann, B. U. (2014). When the brain takes a break: A model-based analysis of mind wandering. *The Journal of Neuroscience*, 34, 16286–16295.
- Mittner, M., Hawkins, G. E., Boekel, W., & Forstmann, B. U. (2016). A neural model of mind wandering. *Trends in Cognitive Sciences*, 20, 570–578.
- Monsell, S. (2003). Task switching. *TRENDS in Cognitive Sciences*, 7(134–140).
- Monsell, S., & Mizon, G. A. (2006). Can the task-cueing paradigm measure an “endogenous” task-set reconfiguration process? *Journal of Experimental Psychology: Human Perception and Performance*, 32, 493–516.
- Newell, A., & Rosenbloom, P. S. (1981). Mechanisms of skill acquisition and the law of practice. In J. R. Anderson (Ed.), *Cognitive skills and their acquisition* (p. 1ñ-55). Hillsdale, NJ: Erlbaum.
- Newell, B. R., & Shanks, D. R. (2014). Unconscious influences on decision making: A critical review. *Behavioral and brain sciences*, 37(1), 1–19.
- Palmeri, T. J. (1999). Theories of automaticity and the power law of practice. *Journal of Experimental Psychology: Learning, Memory, and Cognition*, 25, 543–551.
- Pedersen, M. L., & Frank, M. J. (2020). Simultaneous hierarchical bayesian parameter estimation for reinforcement learning and drift diffusion models: a tutorial and links to neural data. *Computational Brain & Behavior*, 3, 458–471.
- Pedersen, M. L., Frank, M. J., & Biele, G. (2017). The drift diffusion model as the choice rule in reinforcement learning. *Psychonomic bulletin & review*, 24(4), 1234–1251.
- Peruggia, M., Van Zandt, T., & Chen, M. (2002). Was it a car or a cat I saw? an analysis of response times for word recognition. In *Case studies in bayesian statistics* (pp. 319–334). Springer.
- Rae, B., Heathcote, A., Donkin, C., Averell, L., & Brown, S. (2014). The hare and the tortoise: Emphasizing speed can change the evidence used to make decisions. *Journal of Experimental Psychology: Learning, Memory, and Cognition*, 40(5), 1226.
- Ratcliff, R., & Rouder, J. N. (1998). Modeling response times for two-choice decisions. *Psychological Science*, 9(5), 347–356.
- Ratcliff, R., Smith, P. L., Brown, S. D., & McKoon, G. (2016). Diffusion decision model: current issues and history. *Trends in cognitive sciences*, 20(4), 260–281.
- Ratcliff, R., & Van Dongen, H. P. (2011). Diffusion model for one-choice reaction-time tasks and the cognitive effects of sleep deprivation. *Proceedings of the National Academy of Science*, 108, 11285–11290.
- Smallwood, J., & Schooler, J. W. (2015). The science of mind wandering: Empirically navigating the stream of consciousness. *Annual Review of Psychology*, 66, 487–518.
- Stewart, N., Brown, G. D. A., & Chater, N. (2005). Absolute identification by relative judgment. *Psychological Review*, 112, 881–911.
- Stewart, N., & Matthews, W. (2009). Relative judgment and knowledge of the category structure. *Psychonomic Bulletin & Review*, 16, 594–599.
- Terry, A., Marley, A. A. J., Barnwal, A., Wagenmakers, E.-J., Heathcote, A., & Brown, S. D. (2015). Generalising the drift rate distribution for linear ballistic accumulators. *Journal of Mathematical Psychology*, 68, 49–58.
- Tran, M.-N., Scharth, M., Gunawan, D., Kohn, R., Brown, S. D., & Hawkins, G. E. (in press). Robustly estimating the marginal likelihood for cognitive models via importance sampling.

*Behavior Research Methods.*

- Turner, B. M., Sederberg, P. B., Brown, S. D., & Steyvers, M. (2013). A method for efficiently sampling from distributions with correlated dimensions. *Psychological Methods*, 18, 368–384.
- Turner, B. M., Van Zandt, T., & Brown, S. (2011). A dynamic stimulus-driven model of signal detection. *Psychological review*, 118(4), 583.
- Van der Linden, D., Frese, M., & Meijman, T. F. (2003). Mental fatigue and the control of cognitive processes: effects on perseveration and planning. *Acta psychologica*, 113(1), 45–65.
- Vickers, D., & Lee, M. D. (1998). Dynamic models of simple judgments: I. Properties of a self-regulating accumulator module. *Nonlinear Dynamics, Psychology, and Life Sciences*, 2, 169–194.
- Vickers, D., & Lee, M. D. (2000). Dynamic models of simple judgments: II. Properties of a self-organizing PAGAN (parallel, adaptive, generalized accumulator network) model for multi-choice tasks. *Nonlinear Dynamics, Psychology, and Life Sciences*, 4, 1–31.
- Visser, I. (2011). Seven things to remember about hidden markov models: A tutorial on markovian models for time series. *Journal of Mathematical Psychology*, 55(6), 403–415.
- Visser, I., Raijmakers, M. E., & van der Maas, H. L. (2009). Hidden markov models for individual time series. In *Dynamic process methodology in the social and developmental sciences* (pp. 269–289). Springer.
- Voss, A., Rothermund, K., & Voss, J. (2004). Interpreting the parameters of the diffusion model: An empirical validation. *Memory & Cognition*, 32, 1206–1220.
- Wagenmakers, E.-J., Ratcliff, R., Gomez, P., & McKoon, G. (2008). A diffusion model account of criterion shifts in the lexical decision task. *Journal of Memory and Language*, 58(1), 140–159.
- Walsh, M. M., Gunzelmann, G., & Van Dongen, H. P. (2017). Computational cognitive modeling of the temporal dynamics of fatigue from sleep loss. *Psychonomic Bulletin & Review*, 24, 1785–1807.
- Wiecki, T. V., Sofer, I., & Frank, M. J. (2013). HDDM: Hierarchical Bayesian estimation of the drift-diffusion model in Python. *Frontiers in Neuroinformatics*, 7, n/a. doi: 10.3389/fninf.2013.00014.
- Wynton, S. K., & Anglim, J. (2017). Abrupt strategy change underlies gradual performance change: Bayesian hierarchical models of component and aggregate strategy use. *Journal of Experimental Psychology: Learning, Memory, and Cognition*, 43(10), 1630.

## Appendix A

### Additional Figures

Figures A1 to A5 show additional results for the goodness of fit of the Markov switching model and the static LBA model to individual subjects: decision accuracy for Experiment 1 of Wagenmakers et al. (2008), and mean RT and decision accuracy for Forstmann et al. (2008) and Experiment 2 of Wagenmakers et al. (2008).

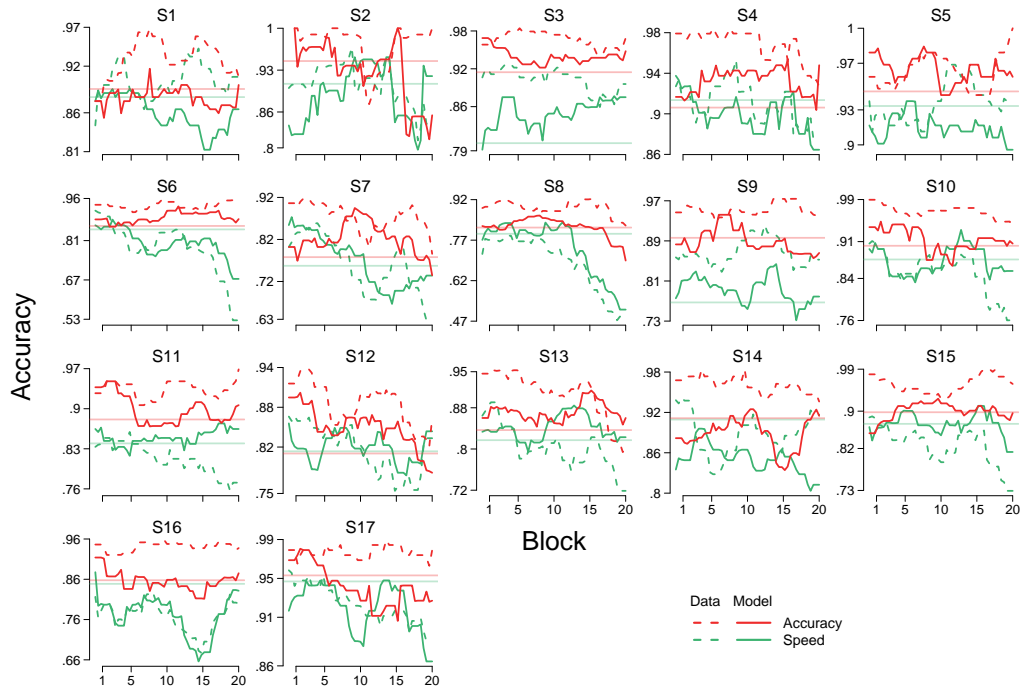


*Figure A1.* Decision accuracy from Experiment 1 of Wagenmakers et al. (2008). Each panel shows a different individual participant. The dashed lines in red and green show performance in the accuracy and speed emphasis conditions, across time-on-task (blocks;  $x$ -axis). The solid lines show the posterior predictive data from the Markov switching model. The straight transparent lines show the posterior predictive data of the static LBA.

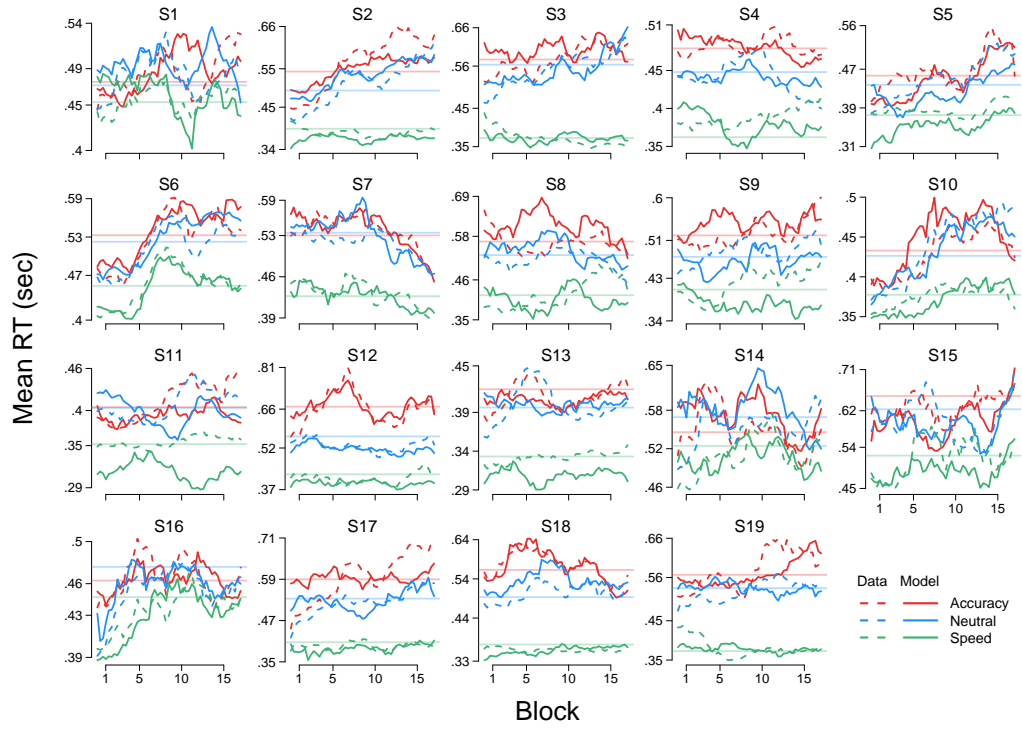


*Figure A2.* Mean RT from Forstmann et al.'s (2008) experiment. Each panel shows a different individual participant. The dashed lines in red, blue and green show performance in the accuracy, neutral and speed emphasis conditions, across time-on-task (blocks;  $x$ -axis). The solid lines show the posterior predictive data from the Markov switching model. The straight transparent lines show the posterior predictive data of the static LBA.

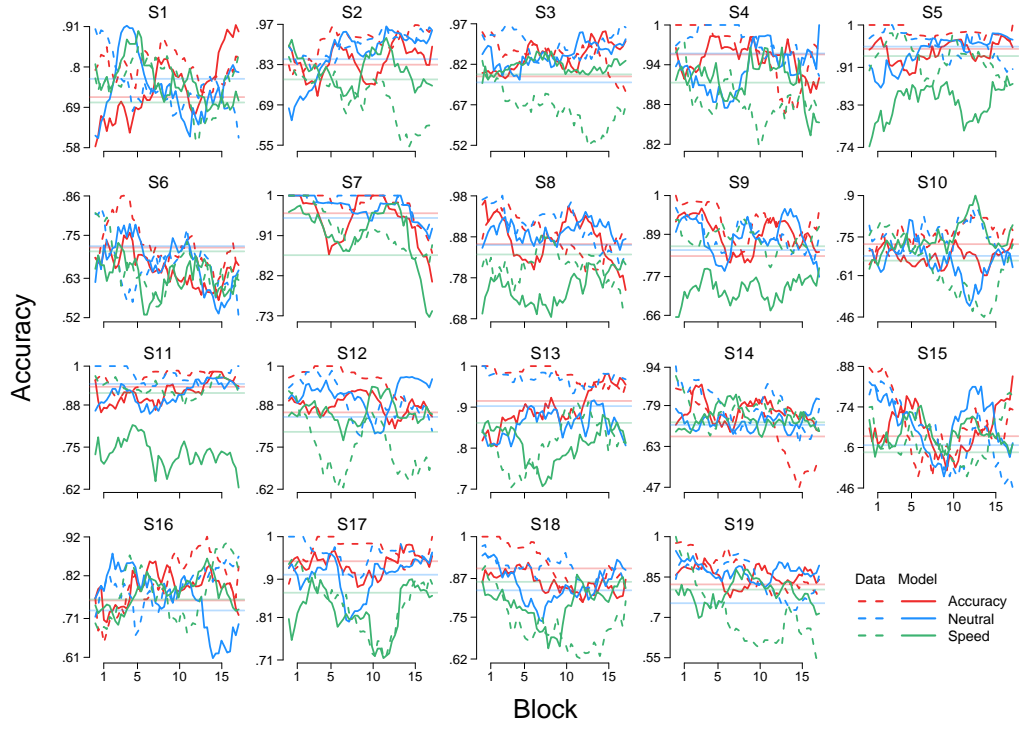


*Figure A3.* Decision accuracy from Forstmann et al.'s 2008 experiment. Each panel shows a different individual participant. The dashed lines in red, blue and green show performance in the accuracy, neutral and speed emphasis conditions, across time-on-task (blocks;  $x$ -axis). The solid lines show the posterior predictive data from the Markov switching model. The straight transparent lines show the posterior predictive data of the static LBA.

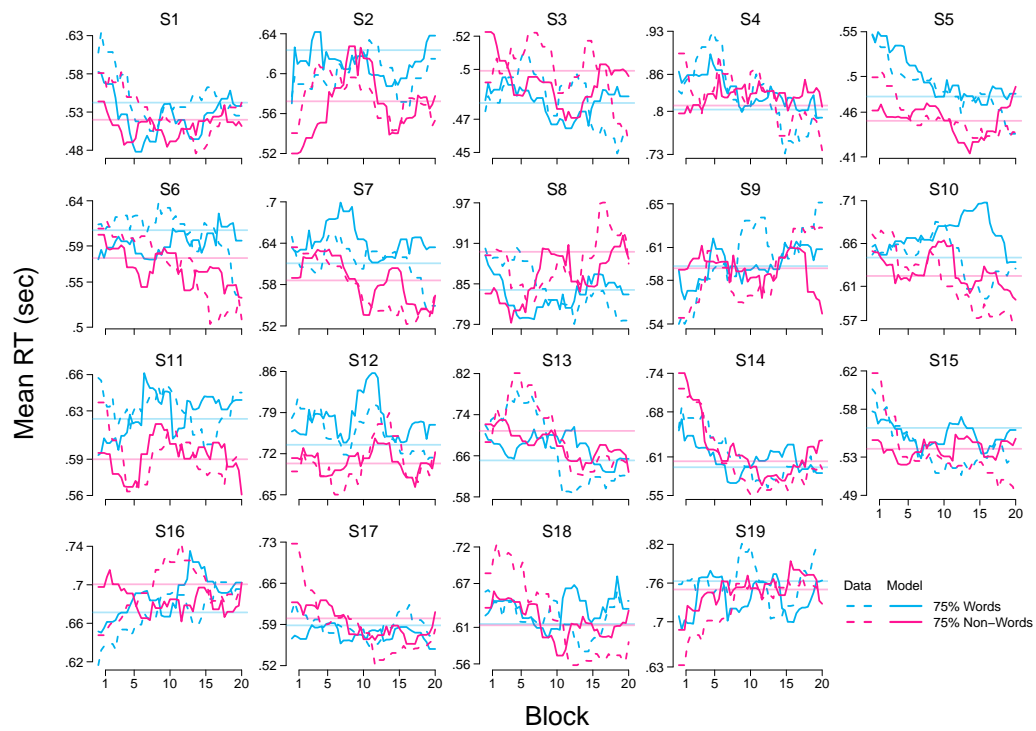


*Figure A4.* Mean RT from Experiment 2 of Wagenmakers et al. (2008). Each panel shows a different individual participant. The dashed lines in blue and pink show performance in the majority word and majority non-word conditions, across time-on-task (blocks;  $x$ -axis). The solid lines show the posterior predictive data from the Markov switching model. The straight transparent lines show the posterior predictive data of the static LBA.

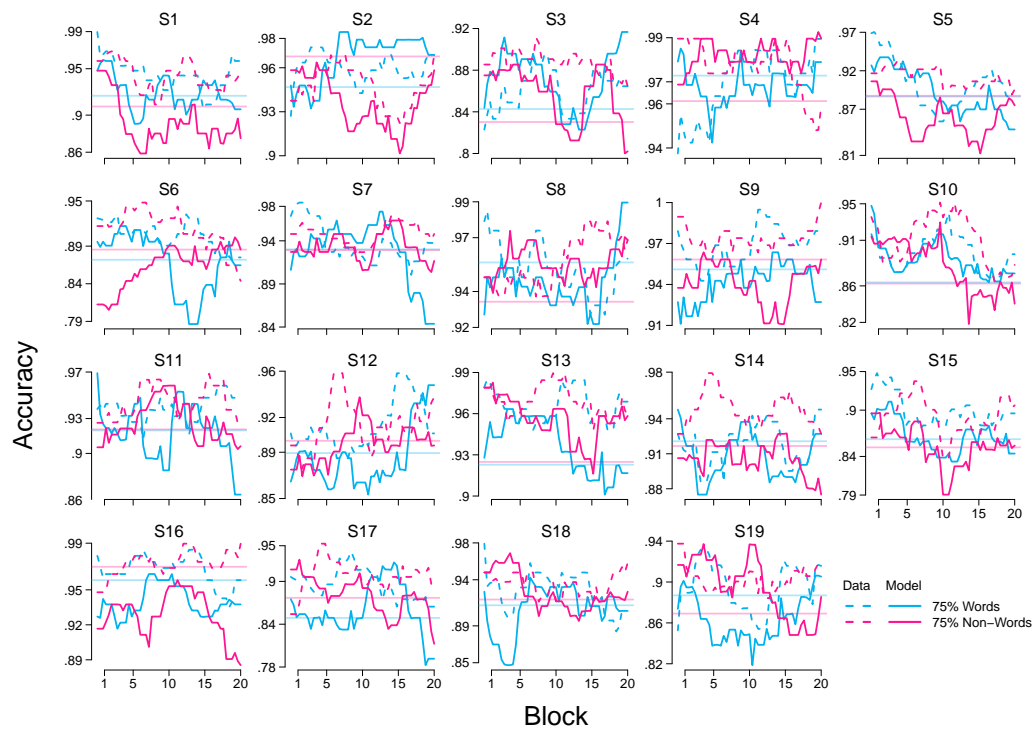


*Figure A5.* Decision accuracy from Experiment 2 of Wagenmakers et al. (2008). Each panel shows a different individual participant. The dashed lines in blue and pink show performance in the majority word and majority non-word conditions, across time-on-task (blocks;  $x$ -axis). The solid lines show the posterior predictive data from the Markov switching model. The straight transparent lines show the posterior predictive data of the static LBA.

## Appendix B

**Bayesian Estimation Methods for AR and Trend Models**

This section develops Bayesian estimation methods for estimating the dynamic AR and trend LBA models based on recent advances in particle MCMC. We first discuss the notation used in the proposed particle MCMC sampling schemes. Let  $\theta \in \Theta \subset \mathbb{R}^{D_\theta}$  be the vector of unknown model parameters and  $p(\theta)$  the prior distribution over  $\theta$ ;  $\mathbb{R}^d$  means  $d$  dimensional Euclidean space. Let  $y_{j,t}$  be the vector of observations for the  $j^{th}$  subject at the  $t^{th}$  block, and define  $y_j := (y_{j,1}, \dots, y_{j,T})$  as the vector of all observations for subject  $j$  and  $y := y_{1:S,1:T} = (y_{1,1:T}, \dots, y_{S,1:T})$  as the vector of observations for all  $S$  subjects. Let  $\alpha_{j,t} \in \chi_\alpha \subset \mathbb{R}^{d_\alpha}$  be the vector of parameter values for subject  $j$  during time period  $t$ . The subject-specific parameters  $\alpha$  are called “random effects”, and the time periods  $t$  are called “blocks”. Let  $\alpha_j := (\alpha_{j,1}, \dots, \alpha_{j,T})$  be all the random effects for subject  $j$  and  $\alpha_{1:S,1:T} := (\alpha_{1,1:T}, \dots, \alpha_{S,1:T})$  the vector of random effects for all  $S$  subjects. For the AR model:

$$p(\alpha_{1:S,1:T}|\theta) = \prod_{j=1}^S p(\alpha_{j,1}|\theta) \prod_{t=2}^T p(\alpha_{j,t}|\alpha_{j,t-1}, \theta)$$

For the trend model:

$$p(\alpha_{1:S,1:T}|\theta) = \prod_{j=1}^S \prod_{t=1}^T p(\alpha_{j,t}|\theta)$$

Equation (1) is the density of  $p(y_{1:S,1:T}|\alpha_{1:S,1:T}, \theta)$ . Our goal is to sample from the posterior density

$$\pi(\theta, \alpha_{1:S,1:T}) := p(y_{1:S,1:T}|\alpha_{1:S,1:T}, \theta) p(\alpha_{1:S,1:T}|\theta) p(\theta) / p(y_{1:S,1:T}), \quad (7)$$

with marginal likelihood

$$p(y_{1:S,1:T}) = \int \int p(y_{1:S,1:T}|\alpha_{1:S,1:T}, \theta) p(\alpha_{1:S,1:T}|\theta) p(\theta) d\theta d\alpha_{1:S,1:T} \quad (8)$$

In addition to sampling from the posterior density (for parameter inference), estimating the marginal likelihood itself is used for model selection via Bayes factors.

We develop a sampling algorithm using particle Markov chain Monte-Carlo, based on the methods from Andrieu, Doucet, and Holenstein (2010). The core idea is to define a target distribution on an augmented space that includes all the parameters of the model (and random effects) as well as the random variables generated by Monte Carlo sampling, and such that this augmented distribution has as its marginal distribution the joint posterior of the parameters and the random effects. Using this target distributions, we derive the particle Metropolis within Gibbs algorithms for the trend and the AR models. One of the attractions of our proposed methods is that essentially the same code and algorithms, with some modifications, can be used to estimate a variety of time-varying random effects models. All that is needed is to code up a new version of the prior distribution of the random effects, as well as the code to generate the group-level parameters. Any Metropolis within Gibbs steps used to generate the group-level parameters are essentially just the standard MCMC updates conditional on the random effects. The estimation of the AR and trend models is discussed in detail below. We also discuss how to modify some parts of the algorithms to estimate a wide range of time-varying random effects models. In addition,

it is straightforward to estimate other dynamic evidence accumulation models (EAMs), for example the diffusion model (Ratcliff et al., 2016). All that is needed is to change the density  $p(y_{1:S,1:T}|\alpha_{1:S,1:T}, \theta)$ .

The rest of the appendix describes the target distributions for the trend and AR models. The novel particle Metropolis-within-Gibbs sampler is then discussed. We also extend the ‘‘Importance Sampling Squared’’ (IS<sup>2</sup>; Tran et al., in press) algorithm for estimating the marginal likelihoods for dynamic LBA models. We suggest that the non-technical reader skips the sections describing the target distributions for different time-varying LBA models.

### Target Distribution for the trend model

This section discusses the augmented target distribution for the polynomial trend model. Let  $\{m_{j,t}(\alpha_{j,t}|\theta, y_{j,t}); j = 1, \dots, S, t = 1, \dots, T\}$  be a family of proposal densities that are used to approximate the conditional posterior densities  $\{\pi(\alpha_{j,t}|\theta); j = 1, \dots, S, t = 1, \dots, T\}$ . Let  $\alpha_{j,t}^{1:R} = (\alpha_{j,t}^1, \dots, \alpha_{j,t}^R)$  refer to all the particles for subject  $j$  generated by a standard Monte Carlo algorithm at block  $t$ . The joint density of the particles given the parameters for subject  $j$  is defined as

$$\psi_j(\alpha_{j,1:T}^{1:R}|\theta) := \prod_{t=1}^T \prod_{r=1}^R m_{j,t}(\alpha_{j,t}^r|\theta); \quad (9)$$

hence the joint density of the particles given the parameters for all subjects is

$$\psi(\alpha_{1:S,1:T}^{1:R}|\theta) = \prod_{j=1}^S \psi_j(\alpha_{j,1:T}^{1:R}|\theta). \quad (10)$$

To define the required augmented target densities, let  $k = (k_1, \dots, k_S)$  and  $k_j = (k_{j,1}, \dots, k_{j,T})$ , with each of  $k_{j,t} \in \{1, \dots, R\}$ ,  $\alpha_{1:S}^{k_{1:S}} = (\alpha_1^{k_1}, \dots, \alpha_S^{k_S})$  be a vector of all selected individual random effects with  $\alpha_j^{k_j} = (\alpha_{j,1}^{k_{j,1}}, \dots, \alpha_{j,T}^{k_{j,T}})$  and  $\alpha_{1:S}^{(-k_{1:S})} = (\alpha_1^{(-k_1)}, \dots, \alpha_S^{(-k_S)})$  with  $\alpha_j^{(-k_j)} = (\alpha_{j,1}^{(-k_{j,1})}, \dots, \alpha_{j,T}^{(-k_{j,T})})$  and  $\alpha_{j,t}^{(-k_{j,t})} = (\alpha_{j,t}^1, \dots, \alpha_{j,t}^{k_{j,t}-1}, \alpha_{j,t}^{k_{j,t}+1}, \dots, \alpha_{j,t}^R)$ .

Consider the augmented target density

$$\tilde{\pi}_R(\alpha_{1:S,1:T}^{1:R}, k_{1:S,1:T}, \theta) = \frac{\pi(\alpha_{1:S,1:T}^{k_{1:S,1:T}}, \theta)}{R^{ST}} \prod_{j=1}^S \frac{\psi_j(\alpha_{j,1:T}^{1:R}|\theta)}{\prod_{t=1}^T m_{j,t}(\alpha_{j,t}^{k_{j,t}}|\theta)}. \quad (11)$$

**Proposition 1.** *The target distribution of Equation 11 has the marginal distribution*

$$\tilde{\pi}_R(\alpha_{1:S,1:T}^{k_{1:S,1:T}}, k_{1:S,1:T}, \theta) = \frac{\pi(\alpha_{1:S,1:T}^{k_{1:S,1:T}}, \theta)}{R^{ST}}; \quad (12)$$

and hence, with some abuse of the notation, we can write  $\tilde{\pi}_R(\alpha_{1:S,1:T}, \theta) = p(\alpha_{1:S,1:T}, \theta|y_{1:S,1:T})$ . The proof follows from Andrieu et al. (2010) and Gunawan, Carter, Fiebig, and Kohn (2017).

### Target Distributions for the AR model

We first briefly describes the generic sequential Monte Carlo (SMC) methods used to approximate the filtering densities  $p(\alpha_{j,t}|y_{j,1:t}, \theta)$  for  $j = 1, \dots, S$  and  $t = 1, \dots, T$ . The SMC algorithm recursively produces a set of weighted particles  $\{\alpha_{j,t}^{(r)}, W_{j,t}^{(r)}\}_{r=1}^R$  at the  $t^{th}$  time period such that

$$\hat{p}(\alpha_{j,t}|y_{j,1:t}, \theta) = \sum_{r=1}^R W_{j,t}^{(r)} \delta_{\alpha_{j,t}^{(r)}}(d\alpha_{j,t}) \quad (13)$$

approximates the density

$$p(\alpha_{j,t}|y_{j,1:t}, \theta) \propto \int p(y_{j,t}|\alpha_{j,t}, \theta) p(\alpha_{j,t}|\alpha_{j,t-1}, \theta) p(\alpha_{j,t-1}|y_{j,1:t-1}, \theta) d\alpha_{j,t-1}; \quad (14)$$

$\delta_a(d\alpha)$  is the Dirac delta distribution located at  $a$ . Equation (14) is used to obtain the particles  $\{\alpha_{j,t}^{(r)}, W_{j,t}^{(r)}\}_{r=1}^R$  by first drawing the particles from a proposal distribution  $m_{j,t}(\alpha_{j,t}|\alpha_{j,t-1}, \theta)$  and then computing the weights

$$w_{j,t}^{(r)} = W_{j,t-1}^{(r)} \frac{p(y_{j,t}|\alpha_{j,t}^{(r)}, \theta) p(\alpha_{j,t}^{(r)}|\alpha_{j,t-1}^{(r)}, \theta)}{m_{j,t}(\alpha_{j,t}^{(r)}|\alpha_{j,t-1}^{(r)}, \theta)}$$

to account for the difference between the posterior density and the proposal density. The weights are then normalized as  $W_{j,t}^{(r)} = w_{j,t}^{(r)} / \sum_{s=1}^R w_{j,t}^{(s)}$ . We implement the SMC algorithm for  $t = 2, \dots, T$  by using a multinomial resampling scheme, denoted as  $\mathcal{M}(a_{j,t-1}^{1:R} | W_{j,t-1}^{1:R})$ . The argument  $a_{j,t-1}^r$  means that  $\alpha_{j,t-1}^{a_{j,t-1}^r}$  is the ancestor of  $\alpha_{j,t}^r$ . Algorithm 1 shows the generic SMC algorithm.

**Algorithm 1** Generic Sequential Monte Carlo AlgorithmInputs:  $y_{j,1:T}$ ,  $R$ ,  $\theta$ Outputs:  $\alpha_{j,1:T}^{1:R}$ ,  $a_{j,1:T-1}^{1:R}$ ,  $w_{j,1:T}^{1:R}$ 1. For  $t = 1$ 

- (a) Sample  $\alpha_{j,1}^r$  from  $m_{j,1}(\alpha_{j,1}|y_{j,1}, \theta)$ , for  $r = 1, \dots, R$
- (b) Calculate the importance weights

$$w_{j,1}^r = \frac{p(y_{j,1}|\alpha_{j,1}^r, \theta) p(\alpha_{j,1}^r|\theta)}{m_{j,1}(\alpha_{j,1}^r|y_{j,1}, \theta)}, r = 1, \dots, R.$$

and normalize those to obtain  $W_{j,1}^{1:R}$ .2. For  $t > 1$ 

- (a) Sample the ancestral indices  $a_{j,t-1}^{1:R} \sim \mathcal{M}(a_{j,t-1}^{1:R}|W_{j,t-1}^{1:R})$ .
- (b) Sample  $\alpha_{j,t}^r$  from  $m_{j,t}(\alpha_{j,t}^r|\alpha_{j,t-1}^{a_{j,t-1}^r}, \theta)$ ,  $r = 1, \dots, R$ .
- (c) Calculate the importance weights

$$w_{j,t}^r = \frac{p(y_{j,t}|\alpha_{j,t}^r, \theta) p(\alpha_{j,t}^r|\alpha_{j,t-1}^{a_{j,t-1}^r}, \theta)}{m_{j,t}(\alpha_{j,t}^r|\alpha_{j,t-1}^{a_{j,t-1}^r}, \theta)}, r = 1, \dots, R.$$

and normalize those to obtain  $W_{j,t}^{1:R}$ .

---

Let  $\alpha_{j,t}^{1:R} = (\alpha_{j,t}^1, \dots, \alpha_{j,t}^R)$  and  $a_{j,t-1}^{1:R} = (a_{j,t-1}^1, \dots, a_{j,t-1}^R)$  refer to all the particles and ancestor indices for subject  $j$ , respectively, generated by the SMC algorithm at block  $t$ . The joint density of the particles given parameters for subject  $j$  is

$$\psi_j(\alpha_{j,1:T}^{1:R}, a_{j,1:T-1}^{1:R}|\theta) = \prod_{r=1}^R m_{j,1}(\alpha_{j,1}^r|\theta) \prod_{t=2}^T \prod_{r=1}^R W_{j,t-1}^{a_{j,t-1}^r} m_{j,t}(\alpha_{j,t}^r|\alpha_{j,t-1}^{a_{j,t-1}^r}, \theta),$$

and the joint density of the particles given the parameters for all subjects is

$$\psi(\alpha_{1:S,1:T}^{1:R}, a_{1:S,1:T-1}^{1:R}|\theta) = \prod_{j=1}^S \psi_j(\alpha_{j,1:T}^{1:R}, a_{j,1:T-1}^{1:R}|\theta).$$

Let  $\alpha_{j,1:T}^{k_{j,1:T}} = (\alpha_{j,1}^{k_{j,1}}, \dots, \alpha_{j,T}^{k_{j,T}})$  be the selected reference trajectory for subject  $j$  with associated indices  $k_{j,1:T}$ . Let  $\alpha_{j,1:T}^{-k_{j,1:T}} = (\alpha_{j,1}^{-k_{j,1}}, \dots, \alpha_{j,T}^{-k_{j,T}})$  denote the collection of all particles for subject  $j$ , except the selected reference trajectory,  $\alpha_{j,1:T}^{k_{j,1:T}}$ . Let  $\alpha_{1:S,1:T}^{k_{1:S,1:T}} =$

$(\alpha_{1,1:T}^{k_{1,1:T}}, \dots, \alpha_{S,1:T}^{k_{S,1:T}})$  be the collection of the selected reference particles for all  $S$  subjects with associated indices  $k_{1:S,1:T} = (k_{1,1:T}, \dots, k_{S,1:T})$ .

**Proposition 2.** *The target distribution is*

$$\tilde{\pi}^R(\alpha_{1:S,1:T}^{1:R}, a_{1:S,1:T-1}^{1:R}, k_{1:S,1:T}, \theta) = \frac{\pi(\alpha_{1:S,1:T}^{k_{1:S,1:T}}, \theta)}{R^{ST}} \quad (15)$$

$$\prod_{j=1}^S \frac{\psi_j(\alpha_{j,1:T}^{1:R}, a_{j,1:T-1}^{1:R} | \theta)}{m_{j,1}(\alpha_{j,1}^{k_{j,1}} | \theta) \prod_{t=2}^T W_{j,t-1}^{a_{j,t-1}^{k_{j,t}}} m_{j,t}(\alpha_{j,t}^{k_{j,t}} | \alpha_{j,t-1}^{a_{j,t-1}^{k_{j,t}}}, \theta)}. \quad (16)$$

This target distribution has the marginal distribution

$$\tilde{\pi}^R(\alpha_{1:S,1:T}^{k_{1:S,1:T}}, k_{1:S,1:T}, \theta) = \frac{\pi(\alpha_{1:S,1:T}^{k_{1:S,1:T}}, \theta)}{R^{ST}}, \quad (17)$$

and hence again, with some abuse of notation, we write  $\tilde{\pi}^R(\alpha_{1:S,1:T}, \theta) = p(\alpha_{1:S,1:T}, \theta | y_{1:S,1:T})$ . The proof follows from Andrieu et al. (2010). The same target distributions apply to a variety of other time-varying models, such as random walk, random walk with drift, and AR plus trend models. The next section describes the proposed particle Metropolis within Gibbs sampling scheme.

## Particle Metropolis within Gibbs Sampling Scheme

Using the target distributions in Equations (11) and (16), we now derive the particle Metropolis within Gibbs algorithms for the trend and AR models. For each component of the sampling scheme, we also explain how to generalise it to other time-varying random effects models. Let  $\theta = (\theta_1, \dots, \theta_H)$  be a partition of the parameter vector into  $H$  components, where each component may be a vector. Algorithm 2 is the general PMwG sampling scheme for dynamic LBA models. The algorithm consists of two main steps: (1) Sampling the group-level parameters conditional on individual level parameters, (2) sampling the individual level parameters conditional on the group-level parameters.

**Algorithm 2** Particle Metropolis within Gibbs for Dynamic LBA models

1. For  $h = 1, \dots, H$

- (a) Sample  $\theta_h^*$  from the proposal  $q_h(\cdot | \alpha_{1:S,1:T}^{k_{1:S,1:T}}, k_{1:S,1:T}, \theta^{(-h)})$ ,
- (b) Accept the proposed values  $\theta_h^*$  with probability

$$\min \left\{ 1, \frac{\tilde{\pi}^R(\theta_h^* | \alpha_{1:S,1:T}^{k_{1:S,1:T}}, k_{1:S,1:T}, \theta^{(-h)}) q_h(\theta_h | \alpha_{1:S,1:T}^{k_{1:S,1:T}}, k_{1:S,1:T}, \theta^{(-h)}, \theta_h^*)}{\tilde{\pi}^R(\theta_h | \alpha_{1:S,1:T}^{k_{1:S,1:T}}, k_{1:S,1:T}, \theta^{(-h)}) q_h(\theta_h^* | \alpha_{1:S,1:T}^{k_{1:S,1:T}}, k_{1:S,1:T}, \theta^{(-h)}, \theta_h)} \right\},$$

2. For  $j = 1, \dots, S$

(a) For the trend model

- i. Sample  $(\alpha_{j,1:T}^{-k_{j,1:T}}) \sim \tilde{\pi}^R(\alpha_{j,1:T}^{-k_{j,1:T}} | \theta, \alpha_{j,1:T}^{k_{j,1:T}}, k_{j,1:T})$  using the conditional Monte Carlo algorithm given in Algorithm 3.
- ii. Sample the index  $k_{j,1:T}$  with probability given by

$$\tilde{\pi}^R(k_{j,1:T} = l_1, \dots, k_{j,T} = l_T | \theta, \alpha_{j,1:T}^{1:R}) = \prod_{t=1}^T W_{j,t}^{l_t}.$$

(b) For the AR model

- i. Sample  $(\alpha_{j,1:T}^{-k_{j,1:T}}, a_{j,1:T-1}^{-k_{j,2:T}}) \sim \tilde{\pi}^R(\alpha_{j,1:T}^{-k_{j,1:T}}, a_{j,1:T-1}^{-k_{j,2:T}} | \theta, \alpha_{j,1:T}^{k_{j,1:T}}, k_{j,1:T})$  using the conditional sequential Monte Carlo given in Algorithm 4.
- ii. Sample  $k_{j,T} = m \sim \tilde{\pi}^R(k_{j,T} | \alpha_{j,1:T}^{1:R}, a_{1:T-1}^{1:R})$ , where  $\tilde{\pi}^R(k_{j,T} | \alpha_{j,1:T}^{1:R}, a_{1:T-1}^{1:R}) \propto W_{j,T}^m$ .
- iii. Sample  $(\alpha_{j,t}^{k_{j,t}}, a_{j,t-1}^{k_{j,t}}) \sim \tilde{\pi}^R(\alpha_{j,t}^{k_{j,t}}, a_{j,t-1}^{k_{j,t}} | \theta, a_{j,1:t-2}^{1:R}, \alpha_{j,1:t-1}^{1:R}, a_{j,t:T-1}^{k_{j,t+1:T}}, \alpha_{j,t+1:T}^{k_{j,t+1:T}}, k_{j,T})$  for  $t = 1, \dots, T$  using Bunch, Lindsten, and Singh (2015) Algorithm

**Discussion of Algorithm 2.** Step 1 of Algorithm 2 samples the group-level parameters  $\theta$  using standard Gibbs or Metropolis within Gibbs steps. These steps are model dependent and need to be derived for each model. We now show the steps to sample the group-level parameters.

**Step 1: Sampling the parameters  $\theta$  for the AR model**

To sample the autoregressive coefficient  $\phi$  from  $\tilde{\pi}^R(\cdot | \alpha_{1:S,1:T}^{k_{1:S,1:T}}, k_{1:S,1:T}, \theta^{(-\phi)})$ , we draw a proposed value  $\phi^*$  from  $\mathcal{N}(\mu_\phi, \sigma_\phi^2)$  truncated within  $(-1, 1)$ , where

$$\sigma_\phi^2 = \left( \sum_{j=1}^S \sum_{t=2}^{T_j} \text{diag}(\alpha_{j,t-1} - \mu)' \Sigma^{-1} \text{diag}(\alpha_{j,t-1} - \mu) \right)^{-1},$$

and

$$\mu_\phi = \sigma_\phi^2 \left( \sum_{j=1}^S \sum_{t=2}^{T_j} \text{diag}(\alpha_{j,t-1} - \mu)' \Sigma^{-1} (\alpha_{j,t} - \mu) \right).$$

Here, and below,  $\text{diag}(x)$  is a diagonal matrix with diagonal elements equal to the vector  $x$ . The candidate is accepted with probability

$$\min \left( 1, \frac{I(-1 < \phi_1^* < 1) \times \dots \times I(-1 < \phi_D^* < 1)}{I(-1 < \phi_1 < 1) \times \dots \times I(-1 < \phi_D < 1)} \right). \quad (18)$$

We sample the  $\mu$  from  $\mathcal{N}(\mu_\mu, \sigma_\mu^2)$ , where

$$\sigma_\mu^2 = \left( S \Sigma^{-1} + \sum_{j=1}^S (T_j - 1) (I - \text{diag}(\phi))' \Sigma^{-1} (I - \text{diag}(\phi)) + I_D \right)^{-1}$$

and

$$\mu_\mu = \sigma_\mu^2 \left( \sum_{j=1}^S \Sigma^{-1} \alpha_{j,1} + \sum_{j=1}^S \sum_{t=2}^{T_j} (I - \text{diag}(\phi))' \Sigma^{-1} \alpha_{j,t} - (I - \text{diag}(\phi))' \Sigma^{-1} \text{diag}(\phi) \alpha_{j,t-1} \right).$$

We sample the covariance matrix  $\Sigma$  from  $IW(v_1, S_1)$ , where  $v_1 = v + \sum_{j=1}^S T_j$  and

$$S_1 = S_\alpha + \sum_{j=1}^S (\alpha_{j,1} - \mu) (\alpha_{j,1} - \mu)' + \sum_{j=1}^S \sum_{t=2}^{T_j} (\alpha_{j,t} - \mu - \text{diag}(\alpha_{j,t-1} - \mu) \phi) (\alpha_{j,t} - \mu - \text{diag}(\alpha_{j,t-1} - \mu) \phi)'$$

### Step 1: Sampling the parameters $\theta$ for the polynomial trend model

We first define  $\mu_t = x_t \beta$ . The matrix  $x_t$  is

$$x_t := \begin{bmatrix} x_{1,t}^\top & 0 & \dots & \dots & 0 \\ 0 & x_{2,t}^\top & \dots & 0 & 0 \\ \vdots & \vdots & \ddots & \dots & \vdots \\ \vdots & \vdots & \vdots & \ddots & \vdots \\ 0 & 0 & \dots & \dots & x_{D,t}^\top \end{bmatrix},$$

and the  $(k_d \times 1)$  vector  $x_{d,t} := (1, t, t^2)^\top$  for  $d = 1, \dots, D$ ,  $\beta := (\beta_1^\top, \dots, \beta_D^\top)^\top$  with  $\beta_d := (\beta_{d,1}, \dots, \beta_{d,k_d})^\top$ .

We sample the parameter  $\beta$  from  $\mathcal{N}(\mu_\beta, \sigma_\beta^2)$ , where

$$\sigma_\beta^2 = \left( \sum_{j=1}^S \sum_{t=1}^T x_t' \Sigma^{-1} x_t + I_D \right)^{-1}$$

and

$$\mu_\beta = \sigma_\beta^2 \left( \sum_{j=1}^S \sum_{t=1}^T x_t' \Sigma^{-1} \alpha_{j,t} \right).$$

We sample the covariance matrix  $\Sigma$  from  $IW(v_1, S_1)$ , where  $v_1 = v + \sum_{j=1}^S T_j$  and

$$S_1 = S_\alpha + \sum_{j=1}^S \sum_{t=1}^{T_j} (\alpha_{j,t} - x_t \beta) (\alpha_{j,t} - x_t \beta)'$$

## Step 2 of the PMwG algorithm

Step 2 of the PMwG in Algorithm 2 is to sample the individual-level parameters for all the subjects for  $j = 1, \dots, S$ ; it is discussed below.

### Trend Model

Step 2a(i) in Algorithm 2 is the conditional Monte Carlo algorithm given in Algorithm 3 that generates  $R - 1$  new particles  $\alpha_{j,1:T}^{-k_{j,1:T}}$ , while keeping the particles  $\alpha_{j,1:T}^{k_{j,1:T}}$  fixed. This step produces a collection of particles  $\alpha_{j,1:T}^{1:R}$ , and (2) the normalised weights  $W_{j,1:T}^{1:R}$ . Step 2a(ii) in Algorithm 2 samples the new index  $k_{j,1:T}$  and updates the selected particles  $\alpha_{j,1:T}^{k_{j,1:T}}$ . Similar steps can be implemented for higher order polynomial trend and spline models. All that is needed to be change is the density  $p(\alpha_{j,t}|\theta)$ . For example,  $p(\alpha_{j,t}|\theta) \sim \mathcal{N}(\mu_t, \Sigma)$ , where the  $d^{th}$  component of  $\mu_t$  is  $\beta_{d1} + \beta_{d2}t + \beta_{d3}t^2 + \beta_{d4}t^3$ ,  $d = 1, \dots, D$ , for the third-degree polynomial trend model.

---

### Algorithm 3 Conditional Monte Carlo Algorithm

---

1. For  $t = 1, \dots, T$

- (a) Sample  $\alpha_{j,t}^r$  from  $m_{j,t}(\alpha_{j,t}|y_{j,t}, \theta)$  for  $r = 1, \dots, R \setminus \{k_{j,t}\}$ .
- (b) Calculate the importance weights

$$w_{j,t}^r = \frac{p(y_{j,t}|\alpha_{j,t}^r, \theta) p(\alpha_{j,t}^r|\theta)}{m_{j,t}(\alpha_{j,t}^r|y_{j,t}, \theta)}, r = 1, \dots, R.$$

- (c) Normalize the weights  $W_{j,t}^r = \frac{w_{j,t}^r}{\sum_{k=1}^R w_{j,t}^k}$ , for  $r = 1, \dots, R$ .
- 

### AR Model

Step 2b(i) in Algorithm 2 is the conditional sequential Monte Carlo step that generates  $R - 1$  particles and ancestor indices while keeping a reference particle  $\alpha_{j,1:T}^{k_{j,1:T}}$  and the associated ancestor indices  $a_{j,1:T-1}^{k_{j,2:T}}$  unchanged.

Algorithm 4 is the conditional sequential Monte Carlo algorithm. The algorithm produces the set of particles  $\alpha_{j,1:T}^{1:R}$ , ancestor indices  $a_{j,1:T-1}^{1:R}$ , and weights  $w_{j,1:T}^{1:R}$ , given the number of particles  $R$ , the group-level parameters  $\theta$ , the dataset for the  $j$ th subject  $y_{j,1:T}$ , the reference particle  $\alpha_{j,1:T}^{k_{j,1:T}}$  and its indices  $k_{j,1:T}$ .

For  $t = 1$ , step (1a) samples the set of particles  $\alpha_{j,1}^r$  for  $r \in \{1, \dots, R\} \setminus \{k_{j,1}\}$ , from the proposal density  $m_{j,1}(\alpha_{j,1}|y_{j,1}, \theta)$ . Step (1b) computes the weights  $w_{j,1}^{1:R}$  and the normalised weights  $W_{j,1}^{1:R}$ . For  $t > 1$ , step (2a) resamples the particles except the reference particle  $\alpha_{j,t}^{k_{j,t}}$  using simple multinomial resampling and obtain the ancestor indices  $a_{j,t-1}^{1:R}$ . Given the resampled particles  $\alpha_{j,t-1}^{a_{j,t-1}^{1:R}}$ , step (2b) generates the set of particles  $\alpha_{j,t}^r$  for  $r \in \{1, \dots, R\} \setminus \{k_{j,t}\}$  from the proposal density  $m_{j,t}(\alpha_{j,t}|\alpha_{j,t-1}^{a_{j,t-1}^r})$ . Step (2c) computes the weights  $w_{j,t}^{1:R}$  and the normalised weights  $W_{j,t}^{1:R}$ .

The conditional sequential Monte Carlo can be applied to a wide range of time-varying models. For any new application, all that is required is the prior densities  $p(\alpha_{1,t}|\theta)$  and  $p(\alpha_{j,t}|\alpha_{j,t-1}, \theta)$ . For the AR model, the density  $p(\alpha_{j,t}|\alpha_{j,t-1}, \theta) \sim N(\mu + \text{diag}(\phi)(\alpha_{j,t-1} - \mu), \Sigma)$  is given in the main text. If we want to use the random walk model, we replace it with the density  $p(\alpha_{j,t}|\alpha_{j,t-1}, \theta) \sim N(\alpha_{j,t-1}, \Sigma)$ .

Steps 2b(ii) and 2b(iii) in Algorithm 2 sample the indices  $k_{j,1:T}$  and update the selected particle  $\alpha_{j,1:T}^{k_{j,1:T}} = (\alpha_{j,1}^{k_{j,1}}, \dots, \alpha_{j,T}^{k_{j,T}})$  using the method developed by Bunch et al. (2015) given in Algorithm 5. Similarly to the conditional sequential Monte Carlo step, this step can be easily modified to estimate a wide range of time-varying random effects models. All that is needed to change is the prior densities  $p(\alpha_{j,1}|\theta)$  and  $p(\alpha_{j,t}|\alpha_{j,t-1}, \theta)$ . The next section discusses the proposal densities used in the PMwG sampler.

### Tuning Parameters and Proposal Densities for the PMwG Sampler

Sampling efficiency greatly increases when appropriate proposal densities are used for the PMwG sampler. For the PMwG sampler, it is necessary to specify the number of particles  $R$ , the proposal densities  $m_{j,1}(\alpha_{j,1}|\theta)$ ,  $m_{j,t}(\alpha_{j,t}|\alpha_{j,t-1}, \theta)$  and  $\omega_{j,t}(\alpha_{j,t}|\alpha_{j,t-1}, \theta)$  for the AR model and  $m_{j,t}(\alpha_{j,t}|\theta)$  for the trend model for  $j = 1, \dots, S$  and  $t = 1, \dots, T$ . The PMwG sampler has three stages: burn-in, initial adaptation, and sampling. It is initialized at a set of parameters  $\theta$  and random effects  $\alpha_{j,1:T}$  for  $j = 1, \dots, S$ . It then proceeds as in Algorithm 2. Initially, for the AR model, in the burn-in and the initial adaptation stages, the proposal density for subject  $j$  is the two component mixture

$$m_{j,1}(\alpha_{j,1}|\theta) = w_{mix}\mathcal{N}(\alpha_{j,1}; \alpha_{j,1}^{(iter-1)}, \epsilon\Sigma_\alpha) + (1 - w_{mix})p(\alpha_{j,1}|\theta), \quad (19)$$

and

$$m_{j,t}(\alpha_{j,t}|\alpha_{j,t-1}, \theta) = w_{mix}\mathcal{N}(\alpha_{j,t}; \alpha_{j,t}^{(iter-1)}, \epsilon\Sigma_\alpha) + (1 - w_{mix})p(\alpha_{j,t}|\alpha_{j,t-1}, \theta), \quad (20)$$

for  $t > 1$ , where  $\alpha_{j,t}^{(iter-1)}$  is the previous iterate  $\alpha_{j,t}^{k_{j,t}}$  for the individual random effects for subject  $j$  at block  $t$ . We set  $w_{mix} = 0.8$  and  $\epsilon$  is a scale factor. In this paper, we set  $\epsilon = 1$ . We apply the proposal density in Equations (19) and (20) for all  $t = 1, \dots, T$ .

**Algorithm 4** Conditional Sequential Monte Carlo algorithm

Inputs:  $N$ ,  $\theta$ ,  $y_{j,1:T}$ ,  $\alpha_{j,1:T}^{k_{j,1:T}}$ , and  $k_{j,1:T}$

Outputs:  $\alpha_{j,1:T}^{1:R}$ ,  $a_{j,1:T-1}^{1:R}$ ,  $w_{j,1:T}^{1:R}$

1. For  $t = 1$

- (a) Sample  $\alpha_{j,1}^r$  from  $m_{j,1}(\alpha_{j,1}|y_{j,1}, \theta)$ , for  $r \in \{1, \dots, R\} \setminus \{k_{j,1}\}$
- (b) Calculate the importance weights

$$w_{j,1}^r = \frac{p(y_{j,1}|\alpha_{j,1}^r, \theta) p(\alpha_{j,1}^r|\theta)}{m_{j,1}(\alpha_{j,1}^r|y_{j,1}, \theta)}, r = 1, \dots, R.$$

and normalize them to obtain  $W_{j,1}^{1:R}$ .

2. For  $t > 1$

- (a) Sample the ancestral indices  $a_{j,t-1}^{-(k_{j,t})} \sim \mathcal{M}(a_{j,t-1}^{-(k_{j,t})}|W_{j,t-1}^{1:R})$ .
- (b) Sample  $\alpha_{j,t}^r$  from  $m_{j,t}(\alpha_{j,t}|\alpha_{j,t-1}^{a_{j,t-1}^r}, \theta)$ ,  $r = 1, \dots, R \setminus \{k_{j,t}\}$ .
- (c) Calculate the importance weights

$$w_{j,t}^r = \frac{p(y_{j,t}|\alpha_{j,t}^r, \theta) p(\alpha_{j,t}^r|\alpha_{j,t-1}^{a_{j,t-1}^r}, \theta)}{m_{j,t}(\alpha_{j,t}^r|\alpha_{j,t-1}^{a_{j,t-1}^r}, \theta)}, r = 1, \dots, R.$$

and normalize to obtain  $W_{j,t}^{1:R}$ .

---

In the sampling stage, the posterior MCMC draws  $(\alpha_{j,1:T}, \theta)$  from the initial adaptation stage are used to build more efficient proposal densities  $m_{j,t}(\alpha_{j,t}|\alpha_{j,t-1}, \theta)$  for the AR model and  $m_{j,t}(\alpha_{j,t}|\theta)$  for the trend model for  $j = 1, \dots, S$  and  $t = 1, \dots, T$ . The posterior draws of the parameters  $\phi$  and  $\Sigma$  for the AR model, and  $\Sigma$  for the trend model, are transformed so that they all lie on the real line. The covariance matrix  $\Sigma$  is reparameterised in terms of its Cholesky factorisation  $\Sigma = LL^T$ , where  $L$  is a lower triangular matrix. We apply a log transformation for the diagonal elements of  $L$ , while the subdiagonal elements of  $L$  are unrestricted. We also the logit transform each element of the vector  $\phi$  to  $\phi_L = \log(\phi/(1-\phi))$ , which lies on the real line. The proposal densities for  $\omega_{j,t}(\alpha_{j,t}|\alpha_{j,t-1}, \theta)$  are the same as  $m_{j,t}(\alpha_{j,t}|\alpha_{j,t-1}, \theta)$  for all  $t > 1$  for the AR model. For the AR model, a multivariate normal distribution is fitted to the posterior draws of  $\alpha_{j,1}$  and  $\theta$  for  $t = 1$  and to the posterior draws of  $\alpha_{j,t}$ ,  $\alpha_{j,t-1}$ , and  $\theta$  for  $t = 2, \dots, T$ ; the conditional distributions  $g(\alpha_{j,1}|\theta) \sim N(\alpha_{j,1}|\mu_{j,1}^{prop}, \Sigma_{j,1}^{prop})$  and  $g(\alpha_{j,t}|\alpha_{j,t-1}, \theta) \sim N(\alpha_{j,t}|\mu_{j,t}^{prop}, \Sigma_{j,t}^{prop})$  are then obtained. The efficient proposal density for subject  $j$  is then the three component

---

---

**Algorithm 5** Conditional Monte-Carlo for the joint ancestor and random effects conditional distributions

---

1. Sample  $(a_{j,t-1}^{(-m)}, \alpha_{j,t}^{(-m)})$  from  $\eta(a_{j,t-1}^{(-m)}, \alpha_{j,t}^{(-m)} | a_{j,t-1}^m, \alpha_{j,t}^m, m)$ ,

$$\eta(a_{j,t-1}^{(-m)}, \alpha_{j,t}^{(-m)} | a_{j,t-1}^m, \alpha_{j,t}^m, m) = \prod_{r \neq m} \frac{v_{j,t-1}^{a_{j,t-1}^r}}{\sum_l v_{j,t-1}^l} \omega_t(\alpha_{j,t}^r | \alpha_{j,t-1}^{a_{j,t-1}^r}),$$

2. Sample index  $m$  from  $\eta(m = m^* | a_{j,t-1}^{1:R}, \alpha_{j,t}^{1:R}) \propto \widetilde{W}_{j,t}^{m^*}$ , where

$$\widetilde{w}_{j,t}^r = \frac{w_{j,t-1}^{a_{j,t-1}^r} p(\alpha_{j,t}^r | \alpha_{j,t-1}^{a_{j,t-1}^r}, \theta) p(y_{j,t} | \alpha_{j,t}^r, \theta) p(\alpha_{j,t+1}^{k_{j,t+1}} | \alpha_{j,t}^r, \theta)}{v_{j,t-1}^{a_{j,t-1}^r} \omega_{j,t}(\alpha_{j,t}^r | \alpha_{j,t-1}^{a_{j,t-1}^r})},$$

if  $v_{j,t} = w_{j,t}$ , then we have that

$$\widetilde{w}_{j,t}^r = \frac{p(\alpha_{j,t}^r | \alpha_{j,t-1}^{a_{j,t-1}^r}, \theta) p(y_{j,t} | \alpha_{j,t}^r, \theta) p(\alpha_{j,t+1}^{k_{j,t+1}} | \alpha_{j,t}^r, \theta)}{\omega_{j,t}(\alpha_{j,t}^r | \alpha_{j,t-1}^{a_{j,t-1}^r})},$$

and  $\widetilde{W}_{j,t}^r = \widetilde{w}_{j,t}^r / \sum_l \widetilde{w}_{j,t}^l$ .

---

mixture

$$m_{j,1}(\alpha_{j,1} | \theta) = w_{1,mix} g(\alpha_{j,1} | \theta) + w_{2,mix} p(\alpha_{j,1} | \theta) + w_{3,mix} \bar{g}(\alpha_{j,1} | \theta), \quad (21)$$

and

$$m_{j,t}(\alpha_{j,t} | \alpha_{j,t-1}, \theta) = w_{1,mix} g(\alpha_{j,t} | \alpha_{j,t-1}, \theta) + w_{2,mix} p(\alpha_{j,t} | \alpha_{j,t-1}, \theta) + w_{3,mix} \bar{g}(\alpha_{j,t} | \alpha_{j,t-1}, \theta), \quad (22)$$

where  $\bar{g}(\alpha_{j,t} | \alpha_{j,t-1}, \theta)$  is also the proposal based on the normal distribution as in  $g(\alpha_{j,t} | \alpha_{j,t-1}, \theta)$  except that we now use  $\alpha_{j,t}^{(iter-1)}$  as the means. Similarly, we fit a multivariate normal distribution to the posterior draws of  $\alpha_{j,t}$  and  $\theta$  as in Equation (21), for all  $t = 1, \dots, T$  for the trend model. Following Hesterberg (1995), including the prior density ensures that the importance weights are bounded if the density  $p(y_{j,t} | \alpha_{j,t}, \theta)$  is bounded, which ensures that the sampler is ergodic. Similar proposals can be used for other time-varying random effects models. The next section discusses the Importance Sampling Squared (IS<sup>2</sup>) method to estimate the marginal likelihood for the time-varying LBA models.

### Estimating the Marginal Likelihood for the dynamic LBA models using Importance Sampling Squared (IS<sup>2</sup>)

The marginal likelihood in Equation (8) is frequently used for Bayesian model selection; see, e.g., Chib and Jeliazkov (2001). We now show how the importance sampling squared (IS<sup>2</sup>) approach can be used to estimate the marginal likelihood of the time-varying LBA models; see Tran et al. (in press) for full details of the IS<sup>2</sup> method. Algorithm 6 outlines the IS<sup>2</sup> algorithm for estimating the marginal likelihood. The unbiased estimate of the likelihood is

$$\hat{p}(y_{1:T}|\theta) = \prod_{t=1}^T \left\{ \frac{1}{R} \sum_{r=1}^R w_{j,t}^{(r)} \right\}.$$

---

**Algorithm 6** Importance Sampling Squared (IS<sup>2</sup>) algorithm for estimating the marginal likelihood

---

For  $i = 1, \dots, M$ ,

1. Generate  $\theta_i \stackrel{iid}{\sim} g_{IS}(\theta)$  and compute the unbiased estimate of the likelihood  $\hat{p}(y_{1:T}|\theta_i) = \prod_{t=1}^T \left\{ \frac{1}{R} \sum_{r=1}^R w_{j,t}^{(r)} \right\}$

2. Compute the weights

$$\tilde{w}(\theta_i) = \frac{\hat{p}(y_{1:T}|\theta_i) p(\theta_i)}{g_{IS}(\theta_i)}.$$

3. The IS<sup>2</sup> estimator of the marginal likelihood  $p(y_{1:T})$

$$\hat{p}_{IS^2}(y) = \frac{1}{M} \sum_{i=1}^M \tilde{w}(\theta_i). \quad (23)$$


---

### Constructing the Proposal Densities

This section outlines how to obtain efficient and reliable proposals: a)  $g_{IS}(\theta)$  for the LBA group-level parameters; b)  $m_{j,1}(\alpha_{j,1}|\theta)$ ,  $m_{j,t}(\alpha_{j,t}|\alpha_{j,t-1}, \theta)$  for the random effects  $\alpha_{j,t}$ ,  $t = 1, \dots, T$  and  $j = 1, \dots, S$  for the AR model; c)  $m_{j,t}(\alpha_{j,t}|\theta)$ ,  $t = 1, \dots, T$  and  $j = 1, \dots, S$  for the random effects  $\alpha_{j,t}$  in the trend model. Our approach to obtain these proposal densities is to run the PMwG sampler for dynamic LBA models to generate efficient posterior samples  $(\alpha_{1:S,1:T}^r, \theta^r)$ ,  $r = 1, \dots, R$ , from the posterior density of the parameters and random effects  $\pi(\theta, \alpha_{1:S,1:T})$ . Given the posterior draws of the group-level parameters  $\theta$ , the proposal density for the parameters  $g_{IS}(\theta)$  is obtained by fitting a mixture of normal densities,

$$g_{IS}(\theta) = \sum_{k=1}^K w_k^{MIX} \mathcal{N}(\theta|\mu_k, \Sigma_k), \quad (24)$$

where  $\mathcal{N}(\mu_k, \Sigma_k)$  denotes the normal pdf with mean  $\mu_k$ , variance-covariance matrix  $\Sigma_k$ , and component weights  $w_k^{MIX}$ . In all our examples, the mixture of normals is fitted using

the Matlab built-in function *fitgmdist*, and  $K$  is set to 2.

Similarly to selecting the proposal densities for  $m_{j,1}(\alpha_{j,1}|\theta)$  and  $m_{j,t}(\alpha_{j,t}|\alpha_{j,t-1}, \theta)$  for the PMwG sampler, a normal distribution is first fitted to the posterior draws of  $\alpha_{j,1}$  and  $\theta$  for  $t = 1$  and to the posterior draws of  $\alpha_{j,t}$ ,  $\alpha_{j,t-1}$ , and  $\theta$  for  $t = 2, \dots, T$  and  $j = 1, \dots, S$ ; we then obtain the conditional distribution  $g(\alpha_{j,1}|\theta) \sim N(\alpha_{j,1}|\mu_{j,1}^{prop}, \Sigma_{j,1}^{prop})$  and  $g(\alpha_{j,t}|\alpha_{j,t-1}, \theta) \sim N(\alpha_{j,t}|\mu_{j,t}^{prop}, \Sigma_{j,t}^{prop})$ . The group level parameters  $\theta$  are appropriately transformed so that they all lie on the real line. The efficient proposal density for subject  $j$  at block  $t$  is the two component mixture

$$m_{j,1}(\alpha_{j,1}|\theta) = w_1^{mix} g(\alpha_{j,1}|\theta) + (1 - w_1^{mix}) p(\alpha_{j,1}|\theta), \quad (25)$$

and

$$m_{j,t}(\alpha_{j,t}|\alpha_{j,t-1}, \theta) = w_1^{mix} g(\alpha_{j,t}|\alpha_{j,t-1}, \theta) + (1 - w_1^{mix}) p(\alpha_{j,t}|\alpha_{j,t-1}, \theta), \quad (26)$$

for  $t > 1$ . The mixture weights are set to  $w_1^{mix} = 0.95$ . For the trend model, the proposal density is

$$m_{j,t}(\alpha_{j,t}|\theta) = w_1^{mix} g(\alpha_{j,t}|\theta) + (1 - w_1^{mix}) p(\alpha_{j,t}|\theta), \quad (27)$$

for all  $t = 1, \dots, T$ . Similar proposals can be used for other time-varying random effects models.

## Appendix C

**Bayesian Estimation Methods for the Markov Switching Model**

This section discusses the proposed Markov Switching LBA model. Let  $y_{i,j} = (RE_{i,j}, RT_{i,j})$  be the observed data for  $i = 1, \dots, N$  trials and  $j = 1, \dots, J$  subjects, where  $RE_{i,j} \in \{1, 2\}$  is the response choice and  $RT_{i,j}$  is the response time for the  $i$ th trial and  $j$ th subject. We assume that, for each subject, the observations  $y_{i,j}$  depend on a hidden discrete stochastic process  $S_{i,j}$  with finite state space  $\{1, \dots, K\}$ . The state switching stochastic process  $S_{i,j}$  is described by the  $(K \times K)$  transition matrix  $\xi_j$ , where  $\xi_{k,l,j} := (\xi_j)_{kl}$  is the transition probability from state  $k$  to state  $l$ :

$$\xi_{k,l,j} = \Pr(s_{i,j} = l | s_{i-1,j} = k), \text{ for all } k, l \in \{1, \dots, K\}. \quad (28)$$

Conditional on knowing the states  $s_j = (s_{1,j}, \dots, s_{N,j})$ , the observations  $y_{i,j}$  are independent. For each trial  $i$ , the distribution of  $y_{i,j}$  depends on one of the  $K$  random effects  $\alpha_j = (\alpha_{1,j}, \dots, \alpha_{K,j})$ :

$$(y_{i,j} | s_{i,j} = k, \alpha_j) \sim LBA(y_{i,j} | \exp(\alpha_{k,j})). \quad (29)$$

To account for the dependence of the random effects in different states, the prior distribution of the vector  $\alpha_j$  is modelled as

$$\alpha_j | \mu, \Sigma \sim N(\alpha_j | \mu, \Sigma). \quad (30)$$

In our applications, the number of states is set to  $K = 2$ . The prior for  $\mu$  is  $N(0, I_D)$ , with  $D$  the dimension of  $\alpha_j$ ; the prior for  $\Sigma$  is Inverse Wishart  $IW(s_0 = I_D, v_0 = 30)$ . The prior for the elements of transition matrix,  $\xi_{1,1,j}$  and  $\xi_{2,2,j}$  are Beta(4, 1) for all  $j$ .

**Bayesian Estimation**

This section develops efficient Bayesian inference for the Markov switching LBA model. Let  $\theta$  be the unknown group-level parameters and  $p(\theta)$  the prior for  $\theta$ . Let  $y_j := (y_{1,j}, \dots, y_{N,j})$  be the vector of observations for the  $j$ th subject and define  $y := y_{1:J} = (y_1, \dots, y_J)$  as the vector of observations for all  $J$  subjects. Let  $\alpha_j := (\alpha_{1,j}, \alpha_{2,j})$  be the vector of random effects for subject  $j$ , and  $p(\alpha_j | \theta)$  its density under the group-level distribution. Now define  $\alpha := \alpha_{1:J} := (\alpha_1, \dots, \alpha_J)$  as the vector of random effects for all  $J$  subjects.

We assume that the random effects  $\alpha_j$  are independent given  $\theta$  and that the observations  $y_{i,j}$  are independent given  $\theta$ ,  $\alpha_j$ ,  $s_j$ , and  $\xi_j$ , i.e.,

$$p(\alpha_{1:J} | \theta) = \prod_{j=1}^J p(\alpha_j | \theta) \text{ and } p(y | \theta, \alpha_{1:J}, s_{1:J}) = \prod_{j=1}^J \prod_{i=1}^N p(y_{i,j} | s_{i,j}, \theta, \alpha_j, \xi_j). \quad (31)$$

The density of the sampling distribution on the state process  $s$  depends only on the transition matrix  $\xi_j$  and is

$$p(s_{1:J} | \xi_{1:J}) = \prod_{j=1}^J p(s_{0,j} | \xi_j) \prod_{i=1}^N p(s_{i,j} | s_{i-1,j}, \xi_j). \quad (32)$$

The goal is to obtain samples from the posterior density

$$p(\alpha_{1:J}, \xi_{1:J}, \theta, s_{1:J} | y_{1:J}) \propto p(y | \theta, \alpha_{1:J}, s_{1:J}) p(s_{1:J} | \xi_{1:J}) p(\alpha_{1:J} | \theta) p(\theta) p(\xi_{1:J})$$

We extend the particle Metropolis within Gibbs (PMwG) sampler of Gunawan et al. (2020) to estimate the Markov switching LBA model. The main requirement of the sampler is to construct an augmented target distribution that includes the discrete states, the model parameters and multiple copies of the random effects and has the required posterior as its marginal.

Let  $\{m_j(\alpha_j | \theta, y_j); j = 1, \dots, S\}$  be the proposal densities used for approximating the conditional densities  $\{p(\alpha_j | \theta, y_j); j = 1, \dots, S\}$ ; see Gunawan et al. (2020) for further details about the proposal densities. Let  $\alpha_j^r$  be the  $r$ th sample from the proposal density  $m_j(\alpha_j | \theta, y_j)$  for subject  $j$ . Define  $\alpha_{1:J}^{1:R} := \{\alpha_1^{1:R}, \dots, \alpha_J^{1:R}\}$  and  $\alpha_j^{1:R} := \{\alpha_j^1, \dots, \alpha_j^R\}$ . The joint density of the particles  $\alpha_{1:J}^{1:R}$  conditional on  $\theta$  and  $y_{1:J}$  is

$$\psi(\alpha_{1:J}^{1:R} | \theta, y) = \prod_{j=1}^J \prod_{r=1}^R m_j(\alpha_j^r | \theta, y_j). \quad (33)$$

Let  $p = (p_1, \dots, p_J)$  with each  $p_j \in \{1, \dots, R\}$ ,  $\alpha_{1:J}^{(-p)} = \{\alpha_1^{(-p_1)}, \dots, \alpha_J^{(-p_J)}\}$ , with  $\alpha_j^{(-p_j)} = (\alpha_j^1, \dots, \alpha_j^{p_j-1}, \alpha_j^{p_j+1}, \dots, \alpha_j^R)$  be the collection of particles excluding the selected particles and  $\alpha_{1:J}^{(p)} = (\alpha_1^{p_1}, \dots, \alpha_J^{p_J})$  be the vector of selected random effects for all  $J$  subjects. The augmented target density is

$$\bar{\pi}_R(\theta, \alpha_{1:J}^{1:R}, s_{1:J}, \xi_{1:J} | y) = \frac{p(\alpha_{1:J}^{1:R}, \theta, s_{1:J}, \xi_{1:J} | y)}{R^S} \frac{\psi(\alpha_{1:J}^{1:R} | \theta, y)}{\prod_{j=1}^S m_j(\alpha_j^{p_j} | \theta, y_j)}. \quad (34)$$

From this target distribution, we can construct the PMwG sampler that generates samples  $(\theta, \alpha_{1:J}^{1:R}, s_{1:J}, \xi_{1:J})$  from the posterior distribution  $p(\alpha_{1:J}, \theta, s_{1:J}, \xi_{1:J} | y)$ . See Gunawan et al. (2020) for further details about the properties of the augmented target densities.

Algorithm 7 describes the PMwG sampling scheme for the hierarchical Markov switching LBA model. The sampler starts at an initial set of group level parameters  $\theta = (\mu, \Sigma)$ , individual random effects  $\alpha_{1:J}$ , the transition matrix  $\xi_{1:J}$ , and the hidden state process  $s_{1:J}$ . Step (2) is the conditional MC algorithm given in Algorithm 3 that generates  $R - 1$  particles while keeping the particles  $\alpha_{1:J}^p$  fixed. The conditional MC algorithm gives the collection of particles  $\alpha_{1:J}^{1:R}$  and the normalised weights  $W_{1:J}^{1:R}$ . Step (3) samples the index vector  $p = (p_1, \dots, p_J)$  with probability given by equation (35). We then update the selected particles  $\alpha_{1:J}^{(p)} = (\alpha_1^{p_1}, \dots, \alpha_J^{p_J})$ , and discard the rest of particles. Step (4) samples the group level parameters using Gibbs steps, conditional on the selected particles  $\alpha_{1:J}^{(p)}$ . Step (5) samples the hidden Markov process  $s_j$ , for  $j = 1, \dots, J$ , using Algorithm 9. Step (6) samples the elements of the transition matrix.

---

**Algorithm 7** PMwG algorithm for the Markov switching LBA model

---

1. Select the initial values for  $s_{1:J}$ ,  $\alpha_{1:J}$ ,  $\xi_{1:J}$ ,  $\theta$  and set  $\alpha_j^1 = \alpha_j^{p_j}$  for  $j = 1, \dots, J$ .
2. Sample  $\alpha_{1:J}^{(-p)} \sim \bar{\pi}_R(\cdot | p, \alpha_{1:J}^p, \theta, y, s_{1:J}, \xi_{1:J})$  using the conditional Monte Carlo algorithm (Algorithm 3).
3. Sample the index vector  $p = (p_1, \dots, p_J)$  with probability

$$\bar{\pi}_R(p_1 = l_1, \dots, p_J = l_J | \alpha_{1:J}^{1:R}, \theta, y, s_{1:J}, \xi_{1:J}) = \prod_{j=1}^J W_j^{l_j}, \quad (35)$$

where  $W_j$  is the normalised weight in Equation (38).

4. Sample the group-level parameters:
    - (a)  $\mu | p, \alpha_{1:J}^p, \xi, y, s_{1:J}, \Sigma$  from  $N(\mu^*, \Sigma^*)$ , where  $\Sigma^* = (J\Sigma^{-1} + I)^{-1}$  and  $\mu^* = \Sigma^* \left( \Sigma^{-1} \sum_{j=1}^J \alpha_j^{p_j} \right)$ .
    - (b)  $\Sigma | p, \alpha_{1:J}^p, \xi, y, s_{1:J}, \mu$  from  $IW(k, B)$ , where  $k = v_0 + J$  and  $B = s_0 + \sum_{j=1}^J \left( \alpha_j^{p_j} - \mu \right) \left( \alpha_j^{p_j} - \mu \right)'$ .
  5. Sample the hidden Markov process  $s_j$  for  $j = 1, \dots, J$  using Algorithm 9.
  6. Sample the elements of the transition matrix. For  $K = 2$ , the transition matrix  $\xi_j$  depends on  $\xi_{1,1,j}$  and  $\xi_{2,2,j}$  for  $j = 1, \dots, J$  subjects.
    - (a) Sample  $\xi_{1,1,j} | p, \alpha_{1:J}^p, \mu, y, s_{1:J}, \Sigma$  from  $\text{Beta}(e_{11} + N_{11,j}^*, e_{12} + N_{12,j}^*)$  for  $j = 1, \dots, J$ , where  $N_{lk,j}^*$  counts the number of transitions from state  $l$  to state  $k$  for subject  $J$ .
    - (b) Sample  $\xi_{2,2,j} | p, \alpha_{1:J}^p, \mu, y, s_{1:J}, \Sigma$  from  $\text{Beta}(e_{21} + N_{21,j}^*, e_{22} + N_{22,j}^*)$  for  $j = 1, \dots, J$ . We set  $e_{11} = e_{22} = 4$  and  $e_{12} = e_{21} = 1$ .
  7. Repeat steps 2 to 6 for the required number of iterations.
-

---

**Algorithm 8** Conditional Monte Carlo (Markov switching) Algorithm
 

---

1. Fix  $\alpha_{1:J}^1 = \alpha_{1:J}^p$
2. For  $j = 1, \dots, J$ 
  - (a) Sample  $\alpha_j^r$  from the proposal density  $m_j(\alpha_j|\theta, y_j)$  for  $r = 2, \dots, R$ .
  - (b) Compute the importance weights

$$w_j^r = \frac{p(y_j|\theta, \alpha_j^r, s_j) p(\alpha_j^r|\theta)}{m_j(\alpha_j^r|\theta, y_j)}, \quad (36)$$

where

$$p(y_j|\theta, \alpha_j^r, s_j) = \prod_{i=1}^N p(y_{i,j}|s_{i,j}, \alpha_{s_{i,j}}^r). \quad (37)$$

- (c) Compute the normalised weights

$$W_j^r = w_j^r / \sum_{k=1}^r w_k^r. \quad (38)$$

.

---

---

**Algorithm 9** Sampling the hidden state process  $s_j$ 


---

1. Run the filtering algorithm and store the filtered state probability  $p(s_{i,j} = k | y_j^i, \alpha_j, \theta, \xi_j)$  for  $k = 1, \dots, K$  and  $i = 1, \dots, N$  trials, where  $y_j^i = (y_{1,j}, \dots, y_{i,j})$ . The following steps are carried out recursively for  $i = 1, \dots, N$

- (a) Compute one-step ahead prediction for  $s_{i,j}$  by using

$$\Pr(s_{i,j} = l | y_j^{i-1}, \alpha_j, \theta, \xi_j) = \sum_{k=1}^K \xi_{k,l,j} \Pr(s_{i-1,j} = k | y_j^{i-1}, \alpha_j, \theta, \xi_j), \quad (39)$$

for  $l = 1, \dots, K$ , where  $\xi_{k,l,j} = \Pr(s_{i,j} = l | s_{i-1,j} = k, y_j^{i-1}, \alpha_j, \theta, \xi_j)$ .

- (b) Filtering for  $s_{i,j}$  by using

$$\Pr(s_{i,j} = l | y_j^i, \theta, \alpha_j, \theta, \xi_j) = \frac{p(y_{i,j} | s_{i,j} = l, y_j^{i-1}, \alpha_j, \theta, \xi_j) \Pr(s_{i,j} = l | y_j^{i-1}, \alpha_j, \theta, \xi_j)}{\sum_{k=1}^K p(y_{i,j} | s_{i,j} = k, y_j^{i-1}, \alpha_j, \theta, \xi_j) \Pr(s_{i,j} = k | y_j^{i-1}, \alpha_j, \theta, \xi_j)}. \quad (40)$$

2. Sample  $s_{N,j}$  from the filtered state probability distribution  $\Pr(s_{N,j} = k | y_j, \theta, \alpha_j, \theta, \xi_j)$ .
3. For  $i = N - 1, N - 2, \dots, 0$ , sample  $s_{i,j}$  from the conditional distribution

$$\Pr(s_{i,j} = k | s_{i+1,j} = l, y_j^i, \theta, \alpha_j, \theta, \xi_j) = \frac{\xi_{k,l,j} \Pr(s_{i,j} = k | y_j^i, \theta, \alpha_j, \theta, \xi_j)}{\sum_{r=1}^K \xi_{r,l,j} \Pr(s_{i,j} = r | y_j^i, \theta, \alpha_j, \theta, \xi_j)}. \quad (41)$$


---